PHILOSOPHICAL TRANSACTIONS OF THE ROYAL SOCIETY A MATHEMATICAL, PHYSICAL & ENGINEERING SCIENCES

A Method of Analysis for Long-Wave Phenomena in the Ocean, Using Electronic Network Models. I. The Earth's Rotation Ignored

S. Ishiguro

Phil. Trans. R. Soc. Lond. A 1959 **251**, 303-340
doi: 10.1098/rsta.1959.0005

A METHOD OF ANALYSIS FOR LONG-WAVE PHENOMENA IN THE OCEAN, USING ELECTRONIC NETWORK MODELS I. THE EARTH'S ROTATION IGNORED

By S. ISHIGURO

National Institute of Oceanography, Wormley, Surrey and Nagasaki Marine Observatory, Nagasaki

(*Communicated by G. E. R. Deacon, F.R.S.—Received* 25 *June* 1958—*Revised* 29 *September* 1958)

[Plate 2]

CONTENTS

A method of analysis for long-wave phenomena in the ocean and examples of its applications are described. A phenomenon to be analyzed is assumed to be 'response' resulting from an 'excitation' on the 'system', and the relations between these are analyzed. The original hydraulic system is divided into a number of cells of finite size. Each cell is assumed to have a constant depth within itself, and is represented by a two-dimensional electric network consisting of many capacitors, which are proportional to the area of the mesh, variable inductors, inversely proportional to the depth of each mesh and variable resistors, proportional to the total energy loss in each mesh. The excitation and its response are represented either by a voltage which represents the water elevation of each mesh or electric current which corresponds to the total flow across each mesh. Complicated cases, like that where the excitation is changing irregularly with both time and two-dimensional space, can be treated by simple and small-scale equipment by applying the reciprocity theorem and the pulse-superposition method.

Vol. 251. A. 996. (Price 14s.)

[Published 19 March 1959

Symbols

Hydraulic system

t	time
T	wave period
λ	wavelength
ω	wave angular velocity
Γ_0, Γ_l	wave amplitudes at point 0, and at distance l from 0
θ_l	phase difference between point 0 and point separated by l from 0
ζ, ζ_0, ζ_1	elevations of free surface above undisturbed level, at arbitrary point, at point 0, and at point separated by l from 0
h	depth of water
x, y	horizontal co-ordinates
l	horizontal distance
Δl	mesh size
$\bar{u}, \bar{v}$	components of mean current velocity from sea surface to bottom, in direction of x and y
u_b, v_b	components of current velocity near sea bottom, in directions of x and y
$\bar{w}_x, \bar{w}_y, \bar{w}$	total flows across vertical section of cell of mesh
F_x, F_y, F	friction coefficients of cell of mesh (dimension T^{-1})
k_F	frictional constant of cell of mesh (dimensionless)
α_l	attenuation constant, at distance l from 0
g	acceleration of gravity

Electrical system

t_e	time
T_e	wave period
c_e	phase velocity of wave propagation
l_e	horizontal distance corresponding to l
x_e, y_e	horizontal co-ordinates corresponding to x and y
i_x, i_y	currents in arms of mesh
ω_e	angular frequency of voltage
$\Delta e_x, \Delta e_y$	voltages across one arm of mesh representing x and y component
e, e_0, e_n	voltages across two terminals of a capacitor of mesh, at arbitrary point, at point 0, and at point separated by n meshes from point 0
E_0, E_n	amplitudes of voltage, at point 0, and at point separated by n meshes from 0
θ_{en}	phase difference of voltage between mesh at point 0 and mesh separated by n meshes from 0
L	inductance of mesh
C	capacitance of mesh
R	resistance of mesh
Z_L	inductive reactance of mesh
Z_C	capacitive reactance of mesh
Z_i	iterative impedance of mesh
α_{en}	attenuation constant, at point separated by n meshes from 0

Common for both systems

K_t coefficient for transformation of time
K_l coefficient for transformation of horizontal distance
K_e coefficient of transformation of water level to voltage
K_i coefficient of transformation of total flow of water to electric current
k ratio of mesh size to wavelength
s coefficient to represent friction term in dimensionless value
ϵ_A error of amplitude in model
ϵ_P error of phase in model
n number of meshes

1. Introduction

Long-wave phenomenon in the ocean can be investigated by ordinary model methods but a great deal of labour, time and money would be required. Some numerical methods based on theoretical equations and using automatic computers can also be used, but here again, a great deal of work would have to be done to set up a programming system for the computers.

The present paper describes an analogue method which uses a variable electric network to treat such problems and their applications. A wide range of conditions can be covered by making only minor variations in the circuit. The author has tried to treat as wide a range of problems as possible by using only simple and small-scale equipment.

2. Basic idea

A phenomenon to be analyzed is assumed to be a 'response' resulting from an 'excitation' on the 'system'. The system is represented by an electric network, and the excitation and the response are represented by some electrical quantities such as voltage or current. Then, when two of them are given, the third (unknown) function can be determined by an operation using the network and these electrical quantities.

Three possible cases, where any one of the elements, system, excitation and response is unknown, and some applications of the operation are shown in table 1.

Table 1

case	element: system	element: excitation	element: response	samples of application
I	known	known	unknown	prediction of phenomenon
II	known	unknown	known	derivation of cause
III	unknown	known	known	representation of system

To carry out this operation easily, these elements should be changeable. It is necessary, however, first to find how these elements can be represented by the network and the electrical quantities. The electric network can then be regarded as both a model of the system and as a computer.

3. Principle of analogy

To represent the three elements, system, excitation and response in a long-wave phenomenon, the following analogy is used between hydraulic and electrical systems.

If the vertical acceleration and the deflecting force due to the earth's rotation are neglected and if it is assumed that the friction force is linearly proportional to the current velocity, the

equations of motion and continuity for the propagation of long waves take the form, assuming unit density:

$$\frac{\partial \bar{u}}{\partial t} = -g\frac{\partial \zeta}{\partial x} - F_x \bar{u}, \tag{1}$$

$$\frac{\partial \bar{v}}{\partial t} = -g\frac{\partial \zeta}{\partial y} - F_y \bar{v}, \tag{2}$$

$$\frac{\partial}{\partial x}(\bar{u}h\,\mathrm{d}y)\,\mathrm{d}x + \frac{\partial}{\partial y}(\bar{v}h\,\mathrm{d}x)\,\mathrm{d}y = -\frac{\partial}{\partial t}\{(\zeta+h)\,\mathrm{d}x\,\mathrm{d}y\}. \tag{3}$$

Assuming

$$\left.\begin{aligned} &\frac{\partial}{\partial t}(\mathrm{d}x) = 0, \quad \frac{\partial}{\partial t}(\mathrm{d}y) = 0, \quad \frac{\partial h}{\partial t} = 0, \quad (\zeta < h), \\ &\mathrm{d}x = \mathrm{d}y \equiv \mathrm{d}l, \quad F_x = F_y \equiv F, \end{aligned}\right\} \tag{4}$$

and introducing the relations

$$\bar{w}_x = \bar{u}h\,\mathrm{d}l, \quad \bar{w}_y = \bar{v}h\,\mathrm{d}l, \tag{5}$$

equations (1), (2), and (3) become

$$\frac{\partial \bar{w}_x}{\partial t} = -gh\,\mathrm{d}l\frac{\partial \zeta}{\partial x} - F\bar{w}_x, \tag{6}$$

$$\frac{\partial \bar{w}_y}{\partial t} = -gh\,\mathrm{d}l\frac{\partial \zeta}{\partial y} - F\bar{w}_y, \tag{7}$$

$$\frac{\partial \zeta}{\partial t} = -\frac{1}{\mathrm{d}l}\left(\frac{\partial \bar{w}_x}{\partial x} + \frac{\partial \bar{w}_y}{\partial y}\right). \tag{8}$$

These equations are to be solved by the analogue method described in this paper. Introducing the following relations

$$t = K_t t_e, \tag{9}$$

$$x, y, l = K_l x_e, K_l y_e, K_l l_e, \tag{10}$$

$$\zeta = K_e e, \tag{11}$$

$$\bar{w}_x, \bar{w}_y = K_i i_x, K_i i_y, \tag{12}$$

equations (6), (7), and (8) become

$$\frac{\partial i_x}{\partial t_e} = -gh\left(\frac{K_e K_t}{K_i}\right)\mathrm{d}l_e\frac{\partial e}{\partial x_e} - K_t F i_x, \tag{13}$$

$$\frac{\partial i_y}{\partial t_e} = -gh\left(\frac{K_e K_t}{K_i}\right)\mathrm{d}l_e\frac{\partial e}{\partial y_e} - K_t F i_y, \tag{14}$$

$$\frac{\partial e}{\partial t_e} = -\left(\frac{K_t K_i}{K_l^2 K_e}\right)\frac{1}{\mathrm{d}l_e}\left(\frac{\partial i_x}{\partial x_e} + \frac{\partial i_y}{\partial y_e}\right). \tag{15}$$

Now, if we design an electric network as shown in figure 1(*b*), we find the following equations:

$$\frac{\partial i_x}{\partial t_e} = -\frac{1}{L}\Delta e_x - \frac{R}{L}i_x, \tag{16}$$

$$\frac{\partial i_y}{\partial t_e} = -\frac{1}{L}\Delta e_y - \frac{R}{L}i_y, \tag{17}$$

$$\frac{\partial e}{\partial t_e} = -\frac{1}{c}(\Delta i_x + \Delta i_y). \tag{18}$$

Assuming

$$\mathrm{d}l_e \frac{\partial e}{\partial x_e} = \Delta e_x, \quad \mathrm{d}l_e \frac{\partial e}{\partial y_e} = \Delta e_y, \tag{19}$$

$$\frac{\partial i_x}{\partial x_e} = \Delta i_x, \quad \frac{\partial i_y}{\partial x_e} = \Delta i_y, \tag{20}$$

$$\mathrm{d}l = \Delta l, \tag{21}$$

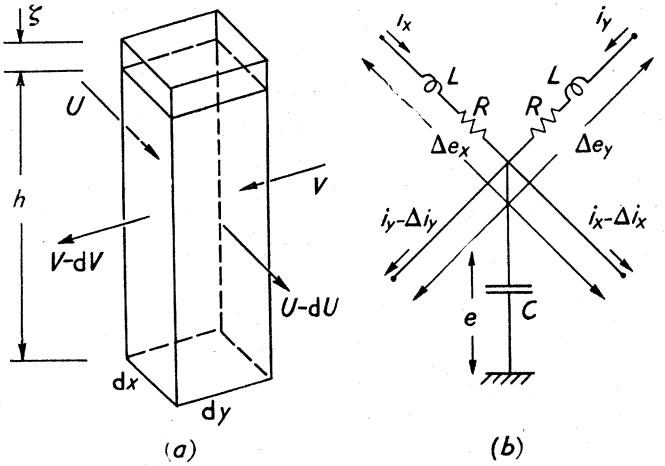

FIGURE 1. Principle of analogy between a hydraulic and an electric system.

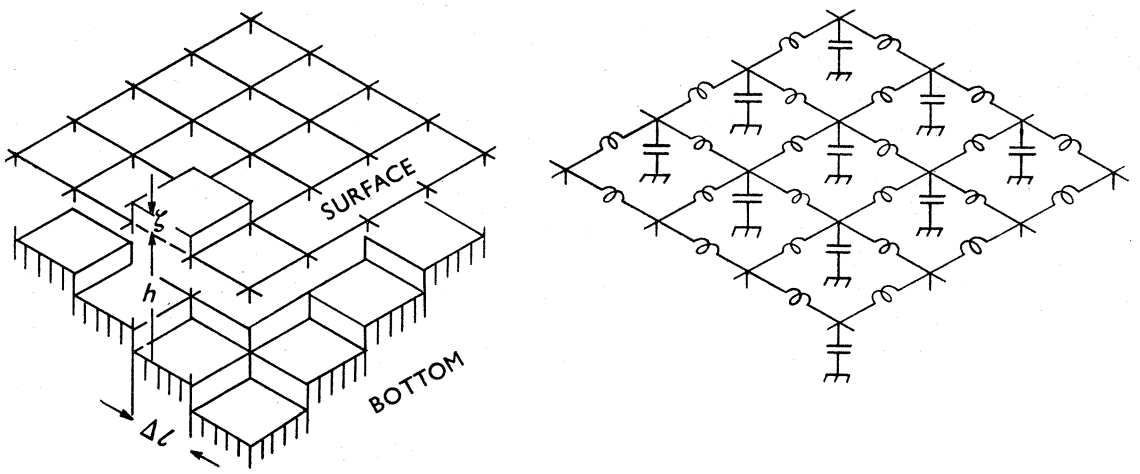

FIGURE 2. Scheme of hydraulic system and a synthesized network model representing it. (The resistors of the network are omitted in the illustration.)

and comparing equations (13), (14) and (15) with equations (16), (17), and (18) respectively we find the following relations:

$$L = \left(\frac{K_i}{K_e K_l}\right)\frac{1}{gh} \quad \text{volts amp}^{-1}\,\text{sec or henries}, \tag{22}$$

$$C = \left(\frac{K_e}{K_i K_l}\right)\Delta l^2 \quad \text{volts}^{-1}\,\text{amp sec or farads}, \tag{23}$$

$$R = \left(\frac{K_i}{K_e}\right)\frac{1}{gh}F \quad \text{volts amp}^{-1}\,\text{or ohms}. \tag{24}$$

PHILOSOPHICAL TRANSACTIONS OF THE ROYAL SOCIETY A MATHEMATICAL, PHYSICAL & ENGINEERING SCIENCES

Then, if a network as shown in figure 2 (*b*), which consists of many networks of type shown in figure 1 (*b*), is set up and the component values are given by equations (22), (23) and (24), it can represent the hydraulic system shown in figure 2 (*b*).

In this model, the elevation of the free surface of the hydraulic system above the undisturbed level is represented by the voltage across the terminals of the capacitor of each unit network, and the total flow through a section of a cell of the hydraulic system is represented by an electric current passing through an arm of the unit network.

4. Error owing to the finite mesh size

An error is introduced in the analogue method because of the finite size of the mesh. This error can be estimated in the simple case where the hydraulic system is sine wave travelling in one dimension in a channel of constant depth, and the corresponding electrical system is an iterative network as shown in figure 3 (*a*). The result can then be extended to more complicated systems.

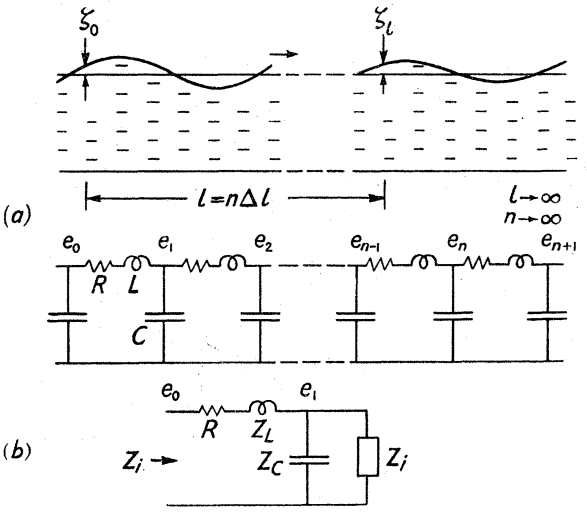

Figure 3. (*a*) Comparison of long-wave propagation in a one-dimensional uniform hydraulic system and an equivalent electric network. (*b*) Equivalent network of one mesh of the above network.

If ζ is uniform along the y-axis, the displacements and voltages can be expressed by

$$\zeta_0 = \Gamma_0 \exp \mathrm{j}\,\omega t, \tag{25}$$

$$\zeta_l = \Gamma_l \exp \mathrm{j}\,(\omega t - \theta_l) = \Gamma_0 \exp -(\alpha_l + \mathrm{j}\,\theta_l) \exp \mathrm{j}\,\omega t, \tag{26}$$

$$e_0 = E_0 \exp \mathrm{j}\,\omega_e t, \tag{27}$$

$$e_n = E_n \exp \mathrm{j}\,(\omega_e t - \theta_{en}) = E_0 \exp -(\alpha_{en} + \mathrm{j}\,\theta_{en}) \exp \omega_e t, \tag{28}$$

where n meshes of the electrical system correspond to a length l in the hydraulic system.

The error in amplitude ϵ_A depends on the difference between the ratio Γ_0/Γ_l and E_0/E_l and the error in phase ϵ_P by the difference between θ_l and θ_{en}. It is convenient to express the errors in the form:

$$\epsilon_A = \frac{\ln (E_n/E_0)}{\ln (\Gamma_l/\Gamma_0)} - 1, \tag{29}$$

$$\epsilon_P = \frac{\theta_{en}}{\theta_l} - 1. \tag{30}$$

It is possible to evaluate ϵ_A and ϵ_P by calculating Γ_0/Γ_l, E_0/E_n, θ_l, and θ_{en} independently. Before proceeding with these calculations, however, it is advisable to express all the constants describing both systems in terms of two non-dimensional constant k and s which are defined below.

As there are n meshes per length l,

$$\Delta l = l/n \tag{31}$$

and if λ is the wavelength

$$\Delta l/\lambda = k. \tag{32}$$

k is thus a measure of the mesh size. If velocity of long-wave propagation is $(gh)^{\frac{1}{2}}$,

$$k = \frac{\omega \Delta l}{2\pi \sqrt{(gh)}}. \tag{33}$$

The constant s is used to represent the frictional term and is given by

$$\frac{F\Delta l}{2\pi \sqrt{(gh)}} = s. \tag{34}$$

Equations (33) and (34) give the constants in the hydraulic system in terms of k and s. The constants in the electrical system can also be expressed in terms of k and s by means of equations (22), (23), and (24) and one obtains

$$k = \frac{\omega_e \sqrt{(LC)}}{2\pi}, \tag{35}$$

$$Z_L = \mathrm{j}\,\omega_e L = 2\pi \mathrm{j}\, k \sqrt{(L/C)}, \tag{36}$$

$$Z_C = \frac{1}{\mathrm{j}\,\omega_e C} = -\mathrm{j}\,\frac{1}{2\pi k}\sqrt{\frac{L}{C}}, \tag{37}$$

$$s = \frac{R}{2\pi}\sqrt{\frac{C}{L}}, \tag{38}$$

$$R = 2\pi s \sqrt{\frac{L}{C}}. \tag{39}$$

Now to return to the hydraulic system. In this simplified case, equations (6), (7), and (8) reduce to

$$\frac{\partial \overline{w}}{\partial t} = -gh\,\mathrm{d}l\,\frac{\partial \zeta}{\partial L} - F\overline{w}, \tag{40}$$

$$\frac{\partial \zeta}{\partial t} = -\frac{1}{\mathrm{d}l}\frac{\partial \overline{w}}{\partial l}, \tag{41}$$

and if the value of ζ_l given by equation (26) is substituted in (40) and (41), and solving by separating real and imaginary parts, one obtains from the real parts

$$\alpha_l = -\ln(\Gamma_l/\Gamma_0) = l\sqrt{\left(\frac{1}{2}\left[\sqrt{\left\{\left(\frac{\omega F}{gh}\right)^2 + \left(\frac{\omega^2}{gh}\right)^2\right\}} - \frac{\omega^2}{gh}\right]\right)}, \tag{42}$$

and from the imaginary parts

$$\theta_l = l\sqrt{\left(\frac{1}{2}\left[\sqrt{\left\{\left(\frac{\omega F}{gh}\right)^2 + \left(\frac{\omega}{gh}\right)^2\right\}} + \frac{\omega^2}{gh}\right]\right)}. \tag{43}$$

If (42) and (43) are expressed in term of k and s:

$$\ln(\Gamma_l/\Gamma_0) = -n\pi\sqrt{[2\{\sqrt{(s^2k^2+k^4)}-k^2\}]}, \tag{44}$$

$$\theta_l = n\pi\sqrt{[2\{\sqrt{(s^2k^2+k^4)}+k^2\}]}. \tag{45}$$

For the electrical system, corresponding values can be obtained by considering a unit mesh of the network for it is immediately apparent from figure 3 (a) that

$$\ln(E_n/E_0) = n\ln(E_1/E_0) \tag{46}$$

and

$$\theta_{en} = n\theta_{e1}. \tag{47}$$

In figure 3 (b) then, if Z_i is the iterative impedance of the network, the impedance of the unit mesh looking from the left is Z_i and thus

$$e_1/e_0 = \frac{Z_C Z_i}{Z_C+Z_i}\Big/Z_i = \frac{1}{1+Z_i/Z_C}. \tag{48}$$

Z_i can be calculated in the usual manner and is equal to

$$Z_i = \tfrac{1}{2}[Z_L+R\pm\sqrt{\{(Z_L+R)^2+4(Z_L+R)\,Z_C\}}], \tag{49}$$

and so, substituting in (49) values of Z_C, Z_L, and R given by (36), (37), and (39), one obtains

$$Z_i = \pi[\mathrm{j}k+s\pm\sqrt{\{s^2-k^2+1/\pi^2+\mathrm{j}s(2k-1/\pi^2k)\}}]\sqrt{(L/C)} \tag{50}$$

and then from (48)

$$e_1/e_0 = \frac{1}{1-2\pi^2k^2+\mathrm{j}2\pi^2k[s\pm\sqrt{\{s^2-k^2+1/\pi^2+\mathrm{j}s(2k-1/\pi^2k)\}}]}. \tag{51}$$

When (51) is reduced to the form $\alpha_{e1}-\mathrm{j}\,\theta_{e1}$ then E_1/E_0 is α_{e1} and the phase shift is θ_{e1}, ϵ_A and ϵ_P can now be evaluated and the full expressions for them are given by equations (52) and (53).

$$\epsilon_A = -1-\frac{1}{\pi\sqrt{[2\{\sqrt{(k^2s^2+k^4)}-k^2\}]}} \times\ln\frac{1}{\sqrt{\left[\left\{1-\pi^2k\left(2k\mp*\sqrt{2}\sqrt{\left[-\left(s^2-k^2+\frac{1}{\pi^2}\right)+\sqrt{\left\{\left(s^2-k^2+\frac{1}{\pi^2}\right)^2+4s^2\left(k-\frac{1}{2\pi^2k}\right)\right\}}\right]}\right)^2\right\} +\pi^4k^4\left(2s+\sqrt{2}\sqrt{\left[\left(s^2-k^2+\frac{1}{\pi^2}\right)+\sqrt{\left\{\left(s^2+k^2+\frac{1}{\pi^2}\right)^2+4s^2\left(k-\frac{1}{2\pi^2k}\right)^2\right\}}\right]}\right)^2\Bigg]} \tag{52}$$

$$\epsilon_P = -1+\frac{1}{\pi\sqrt{[2\{\sqrt{(k^2s^2+k^4)}+k^2\}]}} \times\tan^{-1}\frac{\sqrt{2}\,s+\sqrt{\left[\left(s^2-k^2+\frac{1}{\pi^2}\right)+\sqrt{\left\{\left(s^2-k^2+\frac{1}{\pi_2}\right)^2+4\left(k-\frac{1}{2\pi^2k}\right)^2\right\}}\right]}}{\sqrt{2}\left(k-\frac{1}{2\pi^2k}\right)\mp*\sqrt{\left[-\left(s^2-k^2+\frac{1}{\pi^2}\right)+\sqrt{\left\{\left(s^2-k^2+\frac{1}{\pi^2}\right)+4s^2\left(k-\frac{1}{2\pi^2k}\right)^2\right\}}\right]}}. \tag{53}$$

$$* \;-\text{ for } k<\frac{1}{\pi\sqrt{2}};\quad +\text{ for } k>\frac{1}{\pi\sqrt{2}}.$$

Calculated values of ϵ_A, ϵ_P, $\Gamma_{\Delta l}/\Gamma_0$ and E_1/E_0 for given conditions are shown by the curves in figure 4, and these have been checked in some cases by experimental values as shown by the circles. It can be seen from the curves that for $1/k = 6$ to 7, $\epsilon_A \cong 0{\cdot}1$ and $\epsilon_P \cong 0{\cdot}06$ which is satisfactory for most cases.

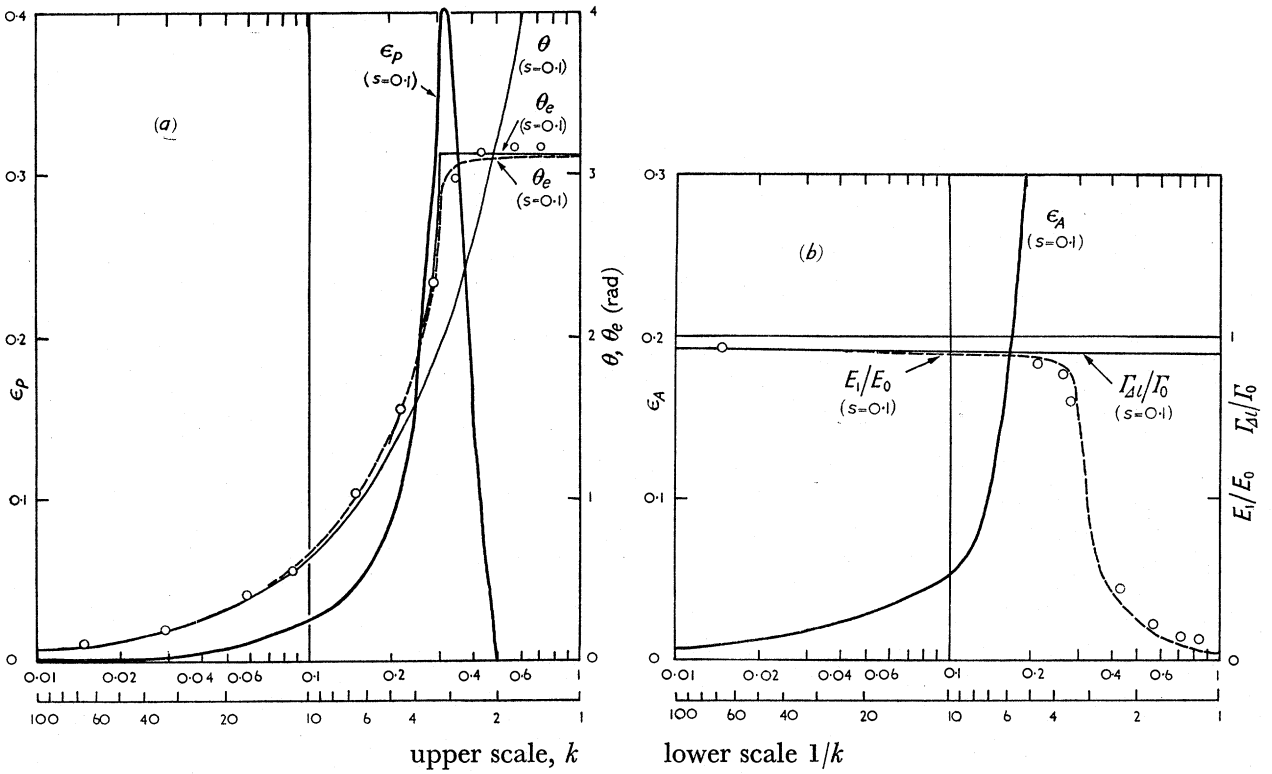

FIGURE 4. (*a*) Example of the values of θ, θ_e, and ϵ_P as a function of k or $1/k$. (*b*) Example of the values of E_1/E_0, $\Gamma_{\Delta l}/\Gamma_0$, and ϵ_A as a function of k or $1/k$. Circles show experimental values obtained under similar conditions.

5. ARRANGEMENTS OF THE NETWORK

5·1. *Value of Q*

In the electric model, all the energy losses in a unit cell of the hydraulic system are represented by the electric resistances which consists of the total value of the self resistances of the inductors and any extra resistances attached. In a case where the energy losses in a hydraulic system are negligible, the electric model has some energy losses, and the lowest limit of this depends mainly on the self resistances of the inductors. This effect causes a greater error in the amplitude of the waves than in the phase.

To reduce this error, inductors which have a high value of Q are required. We can estimate a value of Q to correspond to a given friction term and wave angular velocity in the hydraulic system by the following relation, derived from equations (22) and (24):

$$Q = \omega/F. \tag{54}$$

Although it is difficult to estimate accurately the value of the friction coefficient F in actual cases, an approximate value can be estimated from an equation of the form

$$F = \frac{k_F \mid u_b \mid u_b}{h\bar{u}}, \tag{55}$$

which is derived from the equation of frictional force per unit area, (see, for example, Proudman 1953, p. 303, eq. 3). Values of k_F of about 0·002 have been estimated by means of actual observations by several workers (Bowden 1956; Rossiter 1953). However, in practice,

after the network is constructed, the value of Q of the inductors used should be adjusted to compare with actual observations. For this purpose, it is useful to compare the damping coefficient of free oscillations on the model with that of the actual oscillations, if this is possible.

5·2. *Range and tolerance of the value of the inductances*

A mesh in which the mean depth of the sea (or lake) is assumed to be zero is represented by an open circuit of a terminal of a network, and a mesh in which the mean depth is assumed to be infinitely deep is represented by a short circuit. For other meshes the inductance varies inversely as the depth, so that a wide range of inductance values must be available. It is not practicable to obtain a single component which can be adjusted over the whole range, and it is therefore necessary to use either fixed inductors with values separated by small steps (e.g. twenty steps might be adequate), or a smaller number of inductors variable over a small range of values. In these cases, the largest depth to be modelled by the network should be ascertained first and the smallest value of inductance should correspond to this. If the capacity of the capacitors in the network is known, the coefficient K_t in equation (9) is automatically given.

If an inductor or capacitor used in the network has a change in value of $\mathrm{d}L$ or $\mathrm{d}C$, the change in the phase velocity of waves in the electric model, $\mathrm{d}c_e$, is given by

$$\mathrm{d}c_e \propto \mathrm{d}L/L^{\frac{3}{2}} \quad \text{or} \quad \mathrm{d}c_e \propto \mathrm{d}C/C^{\frac{3}{2}}. \tag{56}$$

It then follows that there should be a finer grading of the lower values of inductance.

5·3. *Determination of the value of the inductances*

To determine the value of an inductance of a network, from equation (22), the mean depth of a mesh must be measured from a chart of the bottom topography. In principle, the mean depth should be measured over a square of centre corresponding to the position of a capacitor, and the corresponding inductances should be divided into four arms of equal inductance as shown in figure 5 (*a*). Therefore, an inductance between the nearest two centres of the meshes P_1 and P_2 should have a value of L_1+L_2, where L_1 and L_2 are the inductances in the arms of the network corresponding to the areas *abcd* and *cdef* in figure 5 (*a*).

An equivalent procedure would be to use the mean depth of an area *ghij* in figure 5 (*b*), to estimate the inductance representing the depth in this area, i.e. an inductance $L_{1\sim2}$ to be connected between the points P_1 and P_2.

Although these considerations are not so important in cases where the mesh size is small in comparison with the variation in bottom topography, the latter procedure is more useful in a case where the mesh size is comparable with the variation, e.g. a case where part of the topography is represented by only one mesh and three of the four arms of the mesh become superfluous as shown in figure 6.

5·4. *Representation of the boundary with an open sea*

When the number of the components of a network is limited, and the area to be modelled is connected with another much wider area (e.g. an open sea), it is desirable to limit the number of components required to represent the wide area. In such a case, it is useful to

connect a group of equivalent impedances across the boundary instead of a complicated network.

The construction of a completely equivalent impedance would, in principle, require almost as large a number of components as the original network. For analyzing one case,

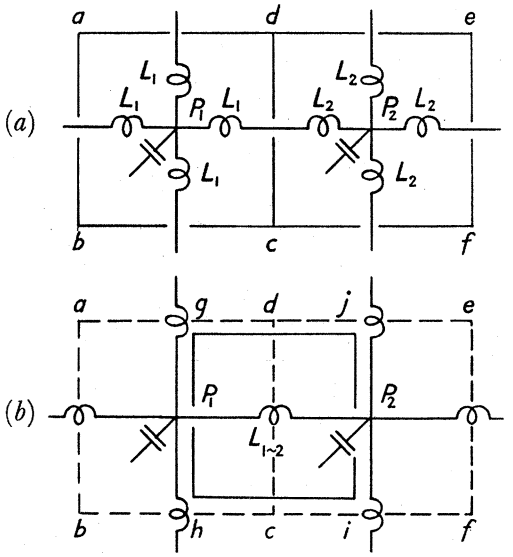

FIGURE 5. Method to determine the value of an inductance corresponding to the mean depth of a mesh.

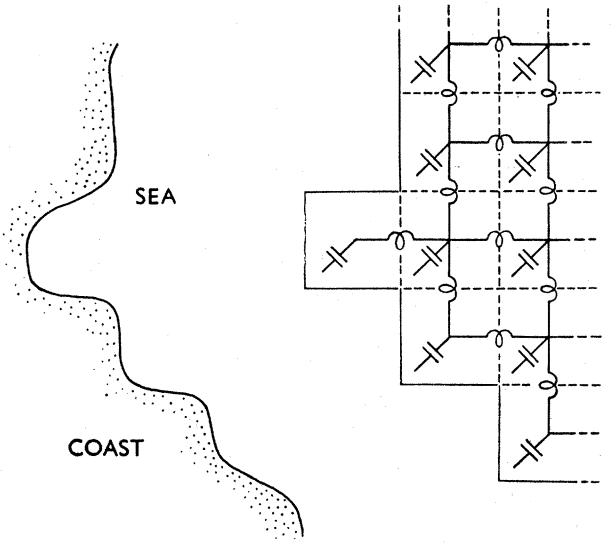

FIGURE 6. Example of a case where the mesh size is small in comparison with the variation in bottom topography.

however, the range of the main component frequency of the waves may not be very wide and so, if a suitable frequency range is chosen, the equivalent impedances can be represented almost entirely by pure resistances. Variable resistors are useful for this purpose and they can be adjusted experimentally by checking the reflexions from them under the same conditions as when in actual use.

PHILOSOPHICAL TRANSACTIONS OF THE ROYAL SOCIETY A MATHEMATICAL, PHYSICAL & ENGINEERING SCIENCES

An example of a network including these equivalent impedances to represent the open sea is shown in figure 7. In this diagram, several steady oscillations caused by the different frequencies in the actual sea form their nodes and antinodes on the same position in the model, shown by an arrow, and this shows that the representation of the boundary by an equivalent impedance is adequate.

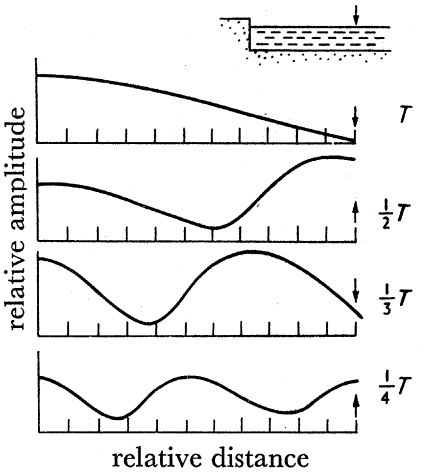

FIGURE 7. Example of a result obtained with a network including equivalent impedances (position is shown by arrow) to represent the open sea.

5·5. *Actual construction and adjustment of the components*

An example of an actual network for a 30-mesh model is shown in figure 8, plate 2. This network consists of sixty variable inductors, sixty variable resistors, thirty fixed capacitors, and several variable resistors for the equivalent impedance.

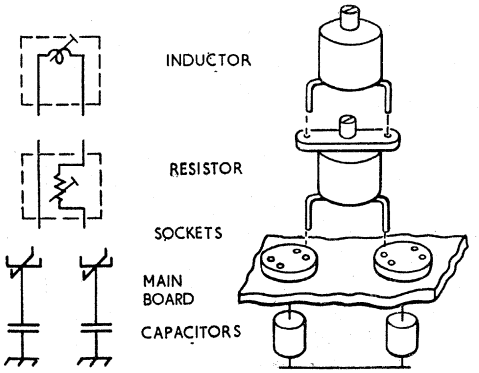

FIGURE 9. Example of the actual arrangement of the network components. Components set between the nearest two sockets are shown.

Experience using this model has suggested that the following specifications would be the most convenient for practical use:

(1) The network is set up on a board and arranged to have a similar shape to the original map of the topography. (This avoids misarrangement.)

(2) The board has sockets to which other components can be plugged in as shown in figure 9.

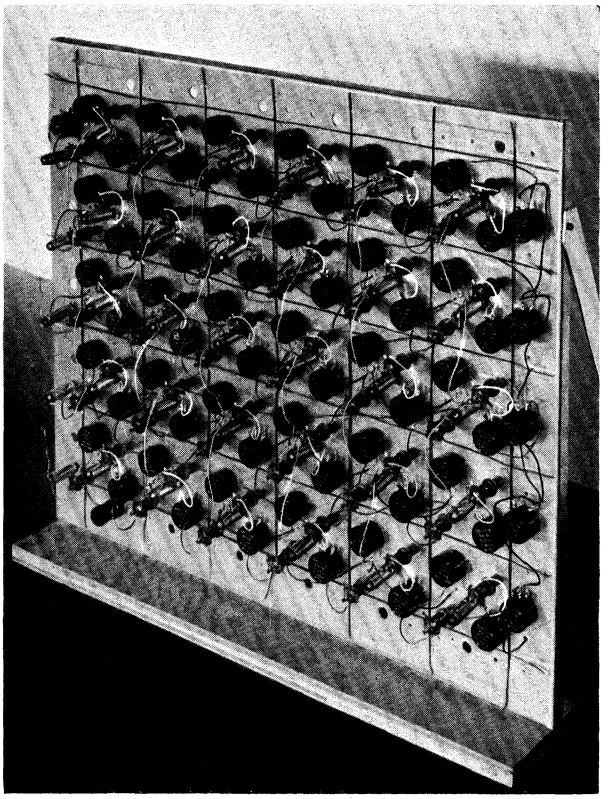

FIGURE 8. Example of a 30-mesh network.

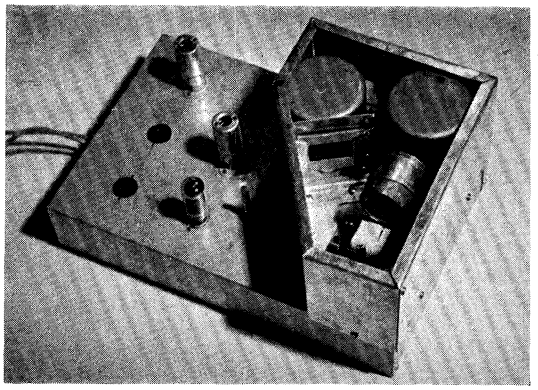

FIGURE 10. Example of an arbitrary waveform generator for a low-frequency range.

(*Facing p.* 314)

PHILOSOPHICAL TRANSACTIONS OF THE ROYAL SOCIETY A MATHEMATICAL, PHYSICAL & ENGINEERING SCIENCES

(3) Inductors which are of the fixed value or variable type can be used with standard pins, i.e. as shown in figure 9.

(4) If the range of the depths to be modelled is not so wide, the capacitors can be all of the same capacitance and can be fixed on the other side of the board, opposite the sockets on which the inductors are set. If several groups of capacitors of different value are required, these should also be of the plug-in type, but in this case, also, it is advisable to have the capacitors set up on the opposite side of the inductors.

(5) If an extra resistor (fixed or variable) is required for an inductor of the network, it should be attached between the inductor and the socket as shown in figure 9.

(6) The inductor and resistor (and capacitor, if necessary), of each component of the network should be measured or adjusted by suitable apparatus when detached from the network.

(7) If the current in arm of the network is required, a standard low resistor should be put between the arm and the socket on the board and the voltage across the resistor should be measured by an oscilloscope.

(8) If equivalent resistors representing the open sea are required, these should use the same type of plug and socket as the other components.

6. Techniques of the analysis

6·1. *Generators and oscilloscope*

To give an excitation to a network model, a generator is required, and to record the response of this excitation, an oscilloscope is also required.

It is desirable that the generator should be stable and able to produce: (1) sine waves, (2) short pulses, and (3) arbitrary waveforms, in a suitable frequency range. It is easier to meet this demand by constructing three separate types of generators.

Although a solution by the analogue method should, in principle, take less than 0·01 s, it is, nevertheless, desirable that the pulse or arbitrary wave should be repeatedly generated so that the response can be recorded more easily on the oscilloscope.

The electrical characteristics of the network should not be altered when the generator and oscilloscope are connected to it. It is therefore essential that the impedance across the generator and oscilloscope terminals should be much higher than that across the terminals of the network to which they are connected.

If the network has been suitably designed, it is easy to obtain the above condition in the case of the oscilloscope because its input impedance (including that of its amplifier) is, in general, very high.

In the case of a generator, however, careful design is necessary, because the output impedance should not be very different from the impedance across the terminals of the network if appreciable electric power is to be fed through, otherwise the effective voltage across the network would be reduced by the mismatching of the impedances. A compromise can be found as follows: (1) Estimation of the lowest permissible impedance, corresponding to the maximum error allowed. (2) Estimation of the maximum voltage required to excite the network, considering the sensitivity of the oscilloscope. (3) Determination of the maximum voltage output of the generator, considering the mismatching of the impedances.

PHILOSOPHICAL TRANSACTIONS OF THE ROYAL SOCIETY A MATHEMATICAL, PHYSICAL & ENGINEERING SCIENCES

As an example the main characteristics of the apparatus at present in use are as follows.

Pulse generator	
pulse length	0·15 to 100 μs
pulse height	20 V max. (at load of 1 kΩ or above)
repetition frequency	50 c/s to 50 kc/s
output impedance	resistance of about 10 kΩ is connected in series with the original output terminal (about 100 times the average characteristic impedance of the present network)
Sine-wave generator	
frequency range	25 c/s to 500 kc/s
accuracy of frequency	$\pm$1 % or $\pm$1 c/s
output voltage	10 V max. (10 Ω) or 1 V max. (75 Ω), or with attenator (600 Ω)
distortion	less than 1 %
Oscilloscope	
two independent beams	
X-axes	
input impedance	1 to 1·5 MΩ, 15 to 20 $\mu\mu$F
frequency response	d.c. to 10 Mc/s: $-$3 dB; 20 Mc/s: $-$12 dB
rise time	0·035 s without overshoot
sensitivity	0·118 V (pk $-pk$)/cm
accuracy of voltage calibration	$\pm$5 % or $\pm$5 mV
accuracy of time calibration	within 2 %
Y-axis	d.c. to 500 kc/s

As an arbitrary waveform generator for this method, electronic photoformers like those used for other electronic analogue computers can be used, if their frequency range and output impedance are suitable. An arbitrary waveform generator of a simple type, suitable for a low-frequency range, has been designed by the author and is shown in figure 10, plate 2. This generator consists of a fixed waveform holder into which a waveform of any shape can be inserted, a photocell, and a scanner which is a rotating optical lever at 120 c/s. This arrangement can generate an arbitrary waveform containing frequency components between 120 and 10 000 c/s.

If the shape of the mask in the photoformer can be varied continuously, it can be used to solve the problems listed under Case II in table 1 (§ 2). An example of a mask of this sort, devised by the author, is shown in figure 11. This mask consists of many thin plates skewered by two rods, and the shape is formed by the edges of the plates and can be changed by a hand operation even when in use. When the output voltage of this mask generator is supplied to a network, the shape is checked at the network terminals by an oscilloscope and adjusted to fit a required waveform and to compensate for any waveform distortion due to the mismatching.

6·2. *Application of the reciprocity theorem to the analysis*

If a network is linear and bilateral, there is a reciprocal relation between the current at one point due to an e.m.f. at a second point and the current at the second point due to an e.m.f. at the first point. Thus in passive, linear electric analogue networks representing

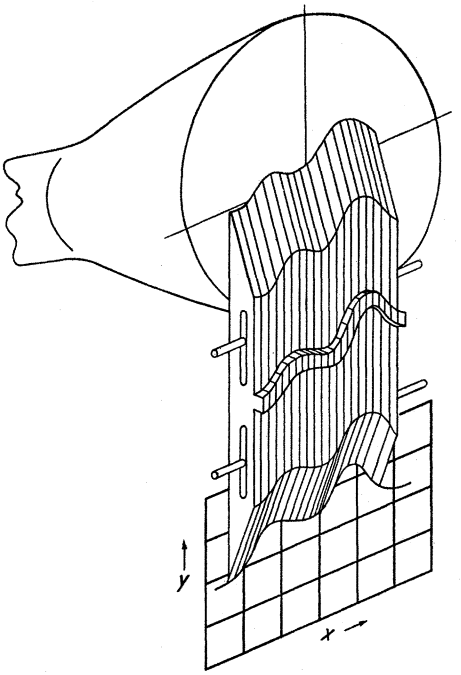

FIGURE 11. Scheme of the variable waveform mask for a photoformer.

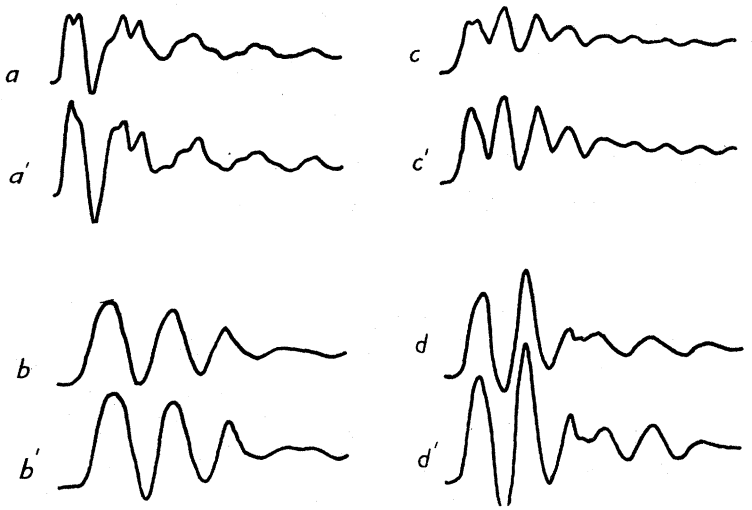

FIGURE 12. Examples of waveform obtained by the reciprocity method in a two-dimensional network model of a lake (Lough Neagh). The relations were obtained between two meshes at different positions in the model.

hydraulic systems, a waveform at a point obtained by injecting an excitation into another point of the mesh is almost the same as the waveform obtained by interchanging these two points. Some examples of waveforms obtained by this method in the case of Lough Neagh are shown in figure 12.

This method is very useful for analyzing cases in which there is more than one input point and a wave of the same form but not of the same amplitude is injected at these points. An example of such a case is the investigation of the free oscillations of Lough

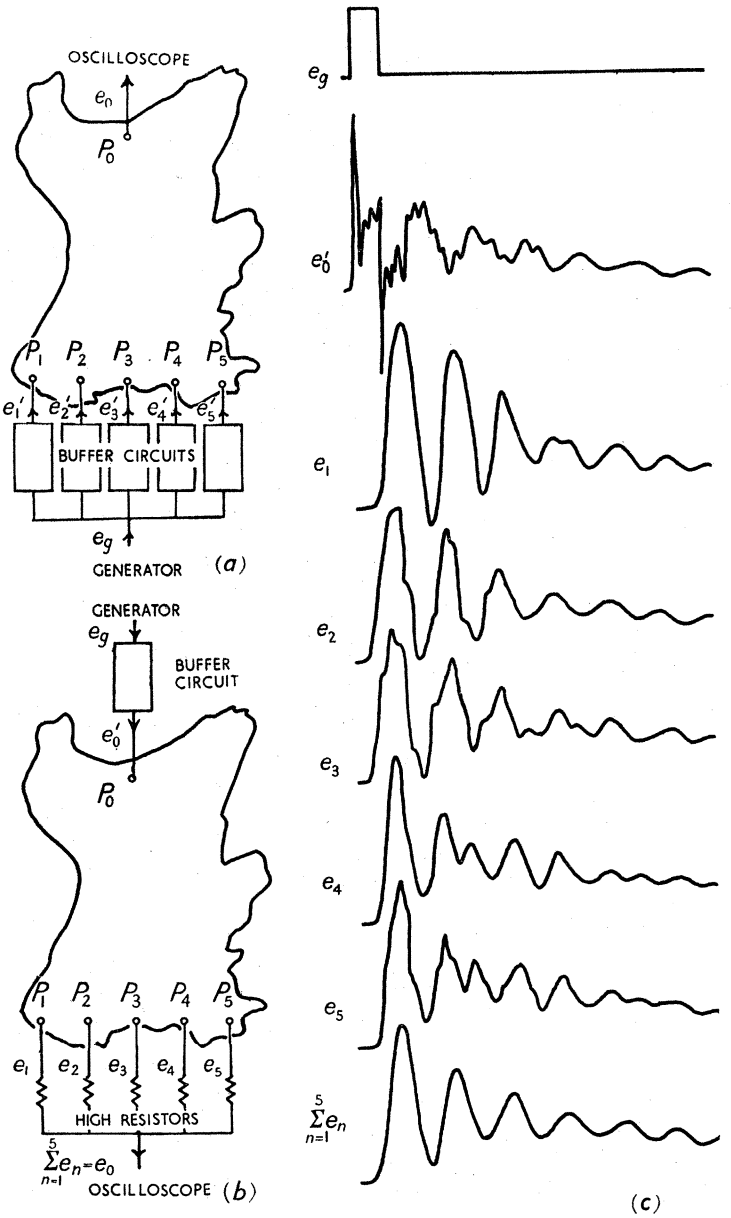

FIGURE 13. Example of the application of the reciprocity method. (*a*) Original arrangement to analyze a free oscillation along the long axis of the lake. (*b*) Equivalent arrangement of (*a*). (*c*) Waveforms in the arrangement (*b*). e_g, Excitation voltage of the generator. e_0', Superposed waveform of the excitation and the response on the point P_0. e_1 to e_5, Responses on the points P_1 to P_5. $\sum_{n=1}^{5} e_n$, Waveform obtained by superposing e_1 to e_5. This waveform is equivalent approximately to that of e_0 in (*a*).

Neagh, shown in figure 13. It is required, here, to obtain the record of the surface level variation at a point P_0 due to a wave advancing from a line $P_1P_2P_3P_4P_5$ as shown in figure 13(*a*). The straightforward method of approach to the problem would be to have

a generator feeding into all the points P_1 to P_5 and measuring the response at P_0 with an oscilloscope. This would be satisfactory in the case of a wave of constant amplitude where the potential at all points is the same, but when the potentials at P_1 to P_5 become different, an alternative connexion is supplied to these points via the generator and the network characteristics are distorted. This effect can only be overcome by installing buffer circuits between the generator and each point. These circuits would complicate the electronic system enormously as each one would require at least one valve or transistor. These complications are avoided by using the reciprocity principle, for then the output of the generator is fed into P_0 and the response at each point P_1 to P_5 is measured in turn when it has been passed on to the oscilloscope through a high resistance of appropriate value for each point. The sum of all the responses gives the required answer. This is shown in figure 13(b). In this method, it is easy to make the value of the resistances high enough to avoid interference and low enough to match the input impedance of the oscilloscope.

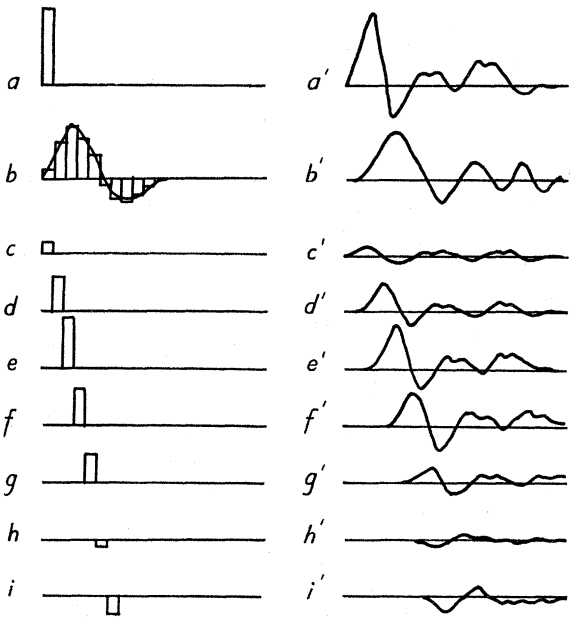

FIGURE 14. Principle of the operation of the pulse superposition method.

6·3. *Pulse superposition method and analogue computer for this method*

Although the method of using an arbitrary waveform generator, described above, is very simple when dealing with waveforms of low frequency, it is not so easy to make a high-quality generator which can be used in a high-frequency range. It is, however, comparatively easy to get a pulse generator and as the network is assumed to be a linear system, a method can be used of synthesizing an arbitrary waveform by the superposition of many pulses.

The method is illustrated in figure 14. When a response on the point of a network, as shown in figure 14(a), called 'unit response', (a'), caused by the injection of a pulse into another point, called 'unit pulse', (a), is solved by the network, we can obtain the response (b') caused by an arbitrary waveform (b) by an operation as follows: (1) Divide the waveform (b) into intervals with the same width as the unit pulse, (c) to (i); (2) Measure the ratio of the height of each of the divided pulses to the height of the unit pulse; (3) Multiply the ratio

with the unit response (taking sign into account), and shift the time axes of these curves, (c') to (i'), according to the position of the pulse. (4) Superpose these curves to obtain (b'). An example of this operation in the case of a V-shaped bay is shown in figure 28. In this diagram, (a) and (b) are an unit pulse and its response, (c) and (d) are a given excitation and its solution.

This operation does not involve as much work as is required to solve the same problem by numerical methods, because the most complicated part of the operation, the obtaining of the response to a unit pulse, is carried out by the network.

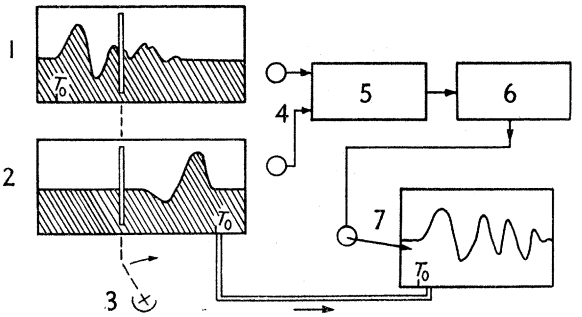

FIGURE 15. Principle of an analogue computer for the superposition method.

However, another electronic analogue method can be made to carry out the superposition operation. Such a method, devised by the author, is shown in figure 15. This device consists of a fixed board (1) (figure 15), a moving board (2), a scanning light beam (3) by which both boards are scanned at a speed high compared with the speed of the moving board, two photocells (4) by which the reflexions of the light beams from the two boards are separately transduced into two electric voltages, an electronic multiplier (5) for these two voltages, an electronic integrator (6) for this multiplied voltage and an output voltage recorder (7) where the movement of the recording chart is geared with the movement of the board (2). If a black-and-white shape representing the waveform of a unit response is put on the board (1) and another representing the waveform to be solved, with the direction of the time axis reversed, is put on the other board (2), the solution of this operation will be obtained on the recording chart.

Although this illustration shows only the principle of the method, it can be modified into a more practical arrangement if necessary.

6·4. *Treatment of excitations and responses*

In general, excitations and their responses on a model network can be treated two-dimensionally. Although it is possible in principle, to solve these cases by using a large number of arbitrary waveform generators and oscilloscopes, the following techniques give the same results using only one generator and oscilloscope.

In these cases it will be convenient to call the area under investigation the 'response area' and the area through which the excitation is introduced the 'excitation area' although in some cases this is reduced to a line.

(A) This is the simplest case already mentioned in § 6·2, that of a plane wave. In this case, as the potential at all points along the wave front is the same, all the corresponding meshes can be connected directly to the generator. The response can be easily obtained in

this case by measuring separately the voltage at each point in the response area by an oscilloscope.

(B) In this case the model is excited through an area or line on which the voltages are in phase but have different amplitudes. This case was also referred to in § 6·2 and it was shown that it could be solved by using the reciprocity principle. In practice, however, it is more convenient to use variable high-resistance potentiometers rather than just high resistances of different value as described in that section.

(C) This is the general case where there is no relation between the voltages at any instant at the points in the excitation area; a solution can be obtained by one of the following two methods.

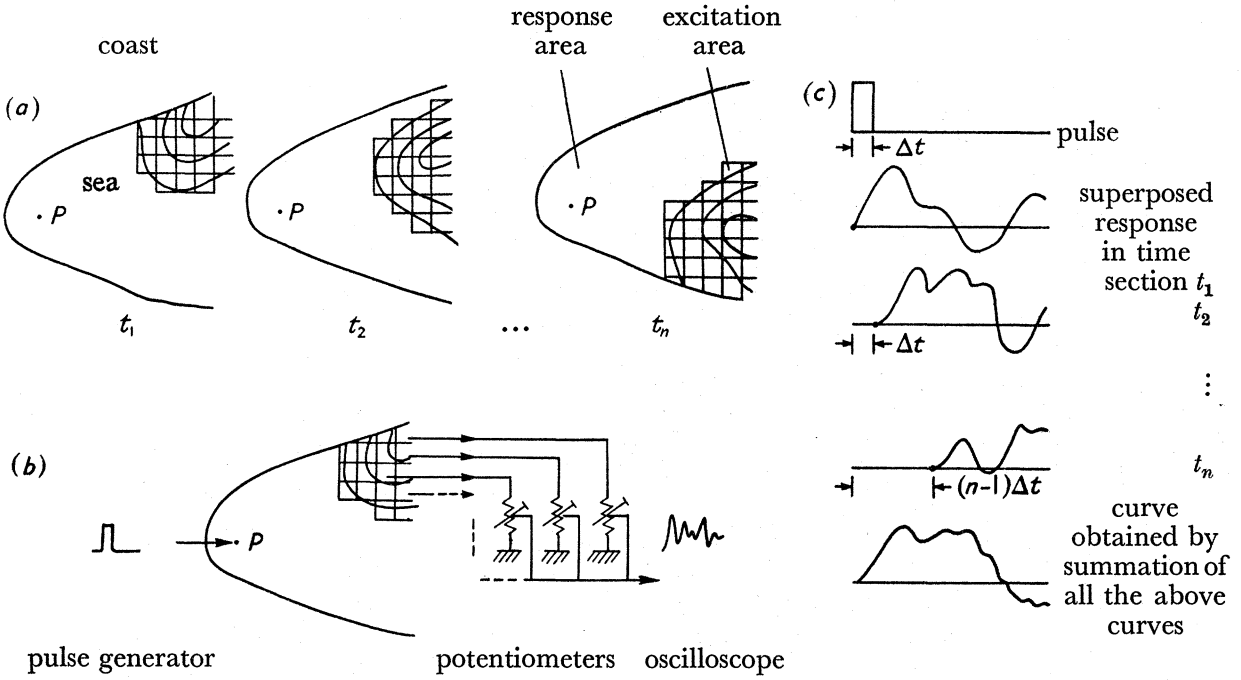

FIGURE 16. Principle of a method (*C*–1), to obtain the response caused by the excitation of a two-dimensional arbitrary waveform, which is changing in time and space

(1) The response at any point in the response area can be obtained by exciting each point in the excitation area in turn with the appropriate waveform and superposing the responses. If the operation is repeated on all the other points in the response area, the two-dimensional solution will be obtained.

(2) The excitation voltages are represented by a set of two-dimensional diagrams spaced at regular time intervals. These are called time sections. For each diagram the mean voltage over each mesh area is worked out as indicated in figure 16(*a*). If a voltage equal to the mean voltage is injected separately into each mesh in turn and the responses on another point *P* in the response area are superposed, the solution is given for this particular time section. This procedure can be simplified considerably in practice by applying the reciprocity method as shown in figure 16(*b*), where many high-resistance potentiometers are used between the meshes and the oscilloscope to represent different voltages. If this operation is repeated for all the time sections required for the problem, and the solutions suitably superposed, the complete solution for the point will be obtained. Some current

has to pass through the potentiometer circuits to make them effective as potentiometers, and this may not be negligible when the number of potentiometers in use is large. This difficulty can be overcome by limiting the number in actual use by carrying out the operations separately for parts of the network for one time section and obtaining the result for the whole network by superposing the responses.

Most actual problems in which an area of sea is excited by a long wave from outside, can be solved by applying method (A) or (B). In this case, the excitation can be represented by a group of voltages fed to a line which divides the response area from the excitation area.

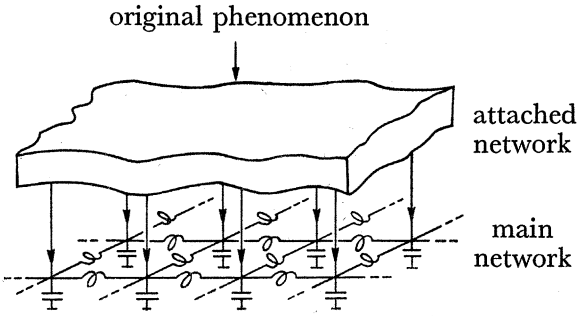

FIGURE 17. Scheme of an attached network to give an equivalent water-level displacement on each mesh corresponding to the effect of a natural cause.

Other cases in which a part of the area to be analyzed is excited directly by a force and the response of another part of this area is required, can be solved by using method (C). In this case, however, the force affecting the sea is usually connected by some relation with the equivalent water-level displacement on each mesh. If this relation is known, the operation can be carried out by making another network to represent this relation. This scheme is shown in figure 17. In all cases, the response is obtained initially as a form of a time function of the voltage on the oscilloscope and the space functions given in the time sections can be synthesized from a large number of these voltage-time responses.

The operation for a case where an excitation is unknown (case II in table 1), can be carried out, in principle, by repeating the operations under many different conditions to give the same response as the given response. It is very useful for this purpose to have a continuously variable waveform generator like that described in § 6·1 which can be changed while in actual use.

6·5. *Spectrum analysis*

When the record of the variation of water level or current is obtained by a network model, the spectrum analysis of the record is sometimes required. This analysis can be carried out by an ordinary manual calculation or by a machine (e.g. an electronic spectrum analyzer). However, in this network model method, the same result can be obtained by a very much simpler procedure.

When the model is repeatedly excited by an arbitrary waveform, the spectrum of the response can be obtained directly, by putting a variable band-pass filter (or an equivalent device) between the network and oscilloscope and measuring the output voltage at various band-pass frequencies. If this operation is carried out on many points on the network, the two-dimensional spectrum is obtained.

If a point on the model is excited by a sine wave of constant amplitude at various frequencies, and the response at another point on the model is measured, a 'frequency response curve' is obtained. If this operation is carried out on many points, a two-dimensional frequency response curve is obtained as shown in the example in figure 34. This can represent the dynamical characteristics of the original hydraulic system and can also be applied to obtain other analyses. For instance, the spectrum of the excitation wave can be obtained from that of the response, if it is known, by dividing by the value at each frequency on response curve, allowing for the calibration. Conversely, but the same procedure, the response spectrum can be derived from the excitation wave spectrum by multiplying this spectrum by the frequency response curve.

7. Examples of applications

7·1. *Oscillation characteristics of a uniform-depth lake (one-dimensional)*

A one-dimensional network model was constructed to investigate the transient state of the oscillations caused by an impulsive force and also steady oscillations in a lake of uniform depth, assuming the friction to be uniformly distributed along the bottom. The principal factors of the model are as follows:

$$n = 30, \quad C = 0{\cdot}05\ \mu\text{F}, \quad L = 0{\cdot}16\ \text{mH}, \quad R = 4\ \Omega,$$
$$\sqrt{(LC)} = 2{\cdot}83\ \mu\text{s}, \quad \sqrt{(L/C)} = 56{\cdot}6\ \Omega, \quad s = 0{\cdot}0113.$$

These values are accurate to within 5 %.

Output impedance of pulse generator = 1 kΩ (approximately).

Output impedance of sine-wave generator = 600 Ω (approximately).

The results are obtained in terms of relative values of time, horizontal distance, and vertical distance of depth. The absolute values can be obtained by using the constants given above and obtaining the values of K_t, K_e and K_i, from equations (22), (23), and (24), assuming a ratio of mesh area to depth.

The water-level variation at each point along the lake is plotted at regular intervals from the start for a total time of about one and a half times the period of the oscillations in figure 18. The water-level variation at each point on the lake is shown as a function of time in figure 19.

In figure 20 are shown stationary waves caused by exciting one end of the lake by sine waves of various frequencies.

7·2. *Oscillation characteristics of a uniform-depth lake, and rectangular lake (two dimensional)*

A two-dimensional model was constructed to investigate two-dimensional stationary waves in a rectangular lake of uniform depth, in which the friction is uniformly distributed over the bottom. The principal factors are as follows:

$$n = 30, \quad C = 0{\cdot}05\ \mu\text{F}, \quad L = 0{\cdot}169\ \text{mH}, \quad R = 3{\cdot}7\ \Omega,$$
$$\sqrt{(LC)} = 2{\cdot}91\ \mu\text{s}, \quad \sqrt{(L/C)} = 58{\cdot}4\ \Omega, \quad s = 0{\cdot}0101.$$

These values are accurate to within 5 %.

The output impedance of the oscillator could be either 75 Ω or 600 Ω, but both values did not have any significant difference on the results.

With all the analyses, stationary sine-wave voltages were used to excite the model, and the results are shown as iso-amplitude lines based on relative values. Absolute values can be obtained asin § 7·1 by using equations (22), (23), and (24). It should be noted that this model does not represent the friction on the side walls of the lake.

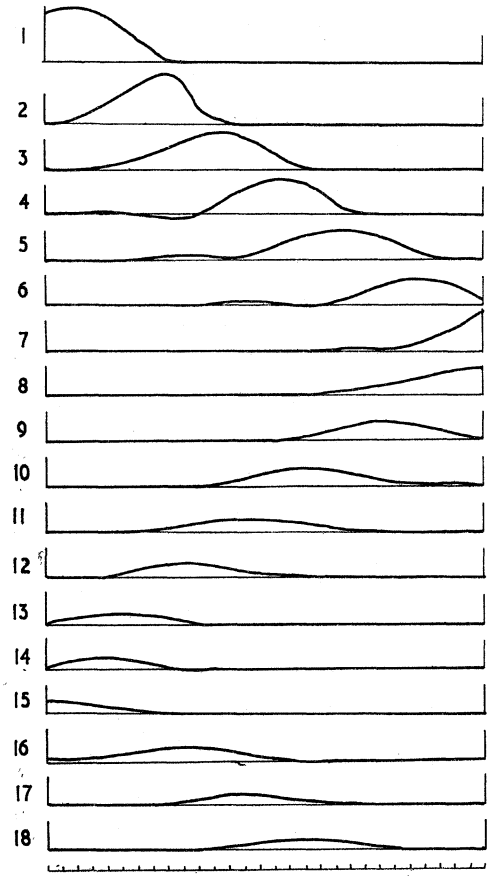

FIGURE 18

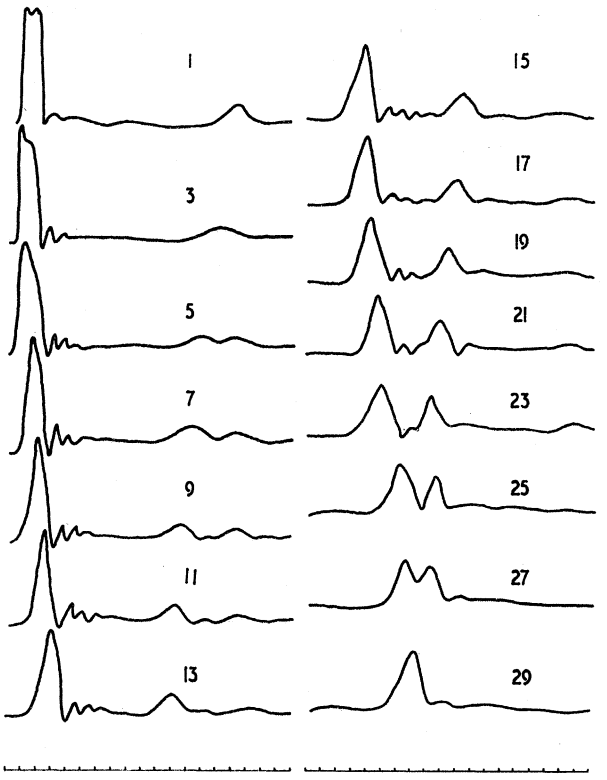

FIGURE 19

FIGURE 18. Transient state of water-level variation caused by a pulse excitation in a lake of uniform depth (one dimensional), with friction. Each diagram is plotted at regular time intervals. Pulse length $= 43 \times 10^{-6}\ K_t$ s.

FIGURE 19. Water-level variation of each point of the lake shown in figure 18. The points are chosen at all the 'odd number' meshes.

A stationary oscillation caused by sending a plane wave along the long axis of the lake is shown in figure 21(*a*). In this analysis, the method described in § 6·4 (A) was applied. Although several positions were taken for the excitation lines, there is very little difference in the results as shown in figure 21(*b*).

The case where a point (shown by an arrow), on the lake is excited by a sine wave of period $14{\cdot}3 \times 10^{-6}\ K_t$ s is shown in figure 22(*a*). Figure 22(*b*) shows the results when the lake is similarly excited by a sine wave of period $7{\cdot}15 \times 10^{-6}\ K_t$ s.

The case where the same lake is excited by a sine wave of period $10{\cdot}0 \times 10^{-6}\ K_t$ s near a corner of the lake (shown by an arrow), is shown in figure 22(*c*).

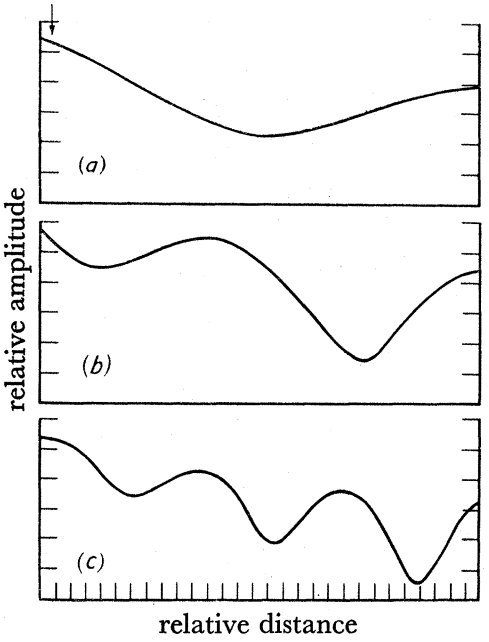

FIGURE 20

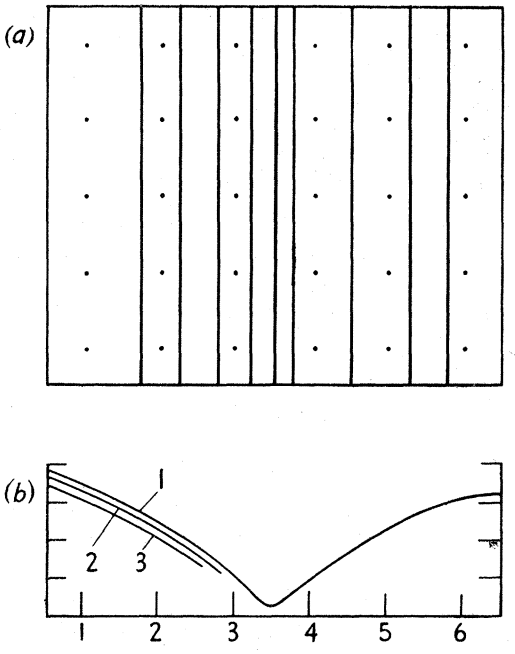

FIGURE 21

FIGURE 20. Stationary waves caused by exciting one end (shown by arrow), of the lake, shown in figure 18 by sine waves. The periods of excitation are: (*a*) $1{\cdot}35 \times 10^{-4}\ K_t$ s, (*b*) $0{\cdot}675 \times 10^{-4}\ K_t$ s, (*c*) $0{\cdot}337 \times 10^{-4}\ K_t$ s.

FIGURE 21. Stationary oscillation caused by sending a plane sine wave in a rectangular lake with friction. (*a*) Iso-amplitude lines. (*b*) Section of the diagram (*a*). Numbers on the lines show that these oscillations are excited at the positions shown by the same numbers on the horizontal axis.

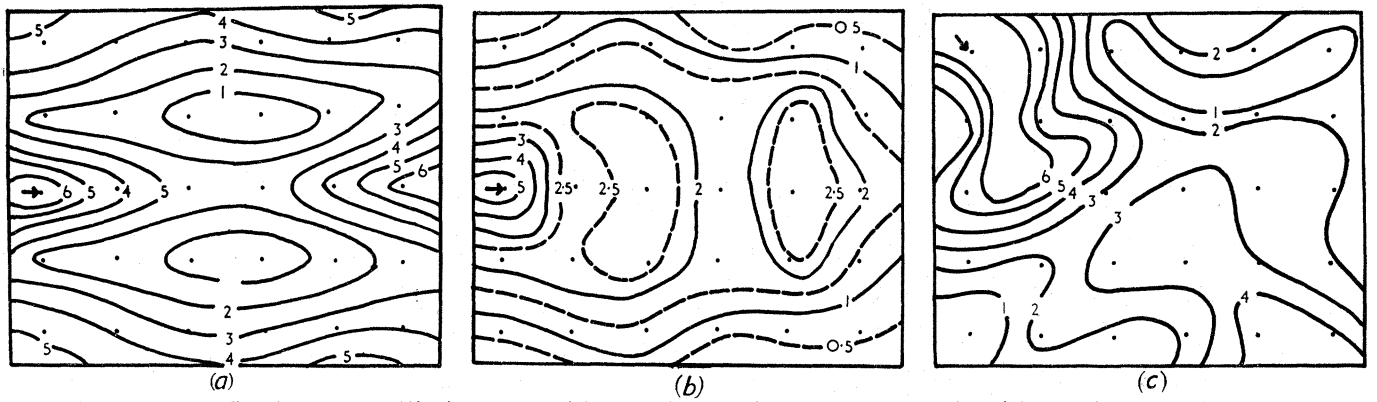

FIGURE 22. Stationary oscillation caused by sending a sine wave to a point (shown by arrow) of the rectangular lake with friction. Lines in the diagram are iso-amplitude lines based on relative values. Period: (*a*) $14{\cdot}3 \times 10^{-6}\ K_t$ s; (*b*) $7{\cdot}15 \times 10^{-6}\ K_t$ s; (*c*) $10{\cdot}0 \times 10^{-6}\ K_t$ s.

7·3. *Oscillation characteristics of a* V*-shaped bay*

A network model is constructed to analyse the case of a V-shaped bay which is disturbed by a pulse-like wave coming from the open sea and also when it is disturbed by stationary waves. The bottom topography of the bay is shown in figure 23 (*a*), it will be observed that the coast is very steep and because of the V shape, the coast line is inclined at an angle to the general direction of the coast line in the neighbourhood. These conditions would give

rise to a great deal of wave reflexion and this effect can be studied with this model. The distribution of the values of depth in the bay and other associated quantities are shown in table 2. In this model, five values of the friction coefficient F are used to correspond to various ranges of depth. The boundary with the open sea is represented by several equivalent impedances which have been adjusted experimentally to the right value, taking into account the output impedance of the pulse generator. Some of the principal factors of this model are as follows:

$$n = 35, \quad C = 0{\cdot}05\ \mu\text{F}, \quad \text{mean depth} = 57{\cdot}8\,\% \text{ of the largest depth},$$

$$\text{mean } L = 0{\cdot}28\ \text{mH}, \quad \text{mean } \sqrt{(L/C)} = 74\ \Omega, \quad \text{mean } \sqrt{(LC)} = 37\,\mu\text{s}, \quad \text{mean } s = 0{\cdot}0086.$$

The results are shown with relative values but they can be applied to real cases by using equations (22), (23), and (24) as was done in §§ 7·1 and 7·2.

TABLE 2

depth (%)	inductance (mH)	resistance (Ω)	number
100	0·158	3·7	5
90	0·175	3·7	4
85	0·186	3·7	1
80	0·198	4·0	2
70	0·225	4·0	2
67	0·236	4·5	5
65	0·243	4·5	2
63	0·250	4·5	2
54	0·293	5·0	1
45	0·351	5·5	1
43	0·368	5·5	2

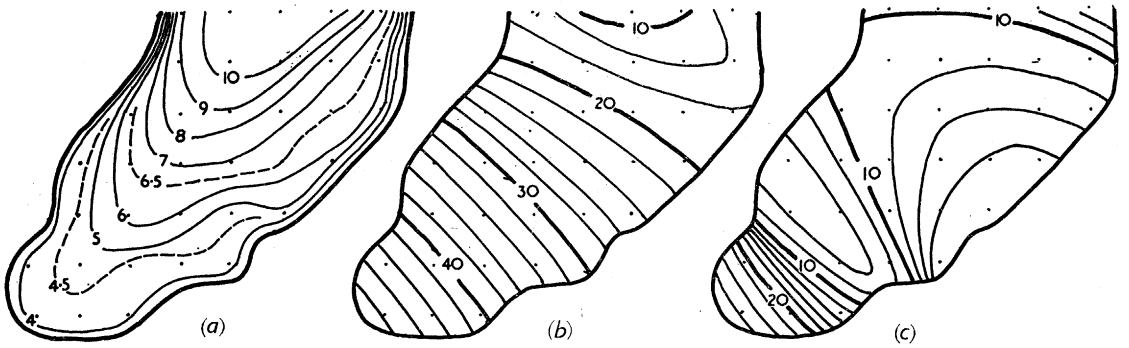

FIGURE 23. (*a*) Bottom topography of the bay used for analysis. Depth is shown by relative values, using 100 for the deepest point. (*b*) Stationary oscillations excited by a sine wave of period $0{\cdot}909 \times 10^{-3}\ K_t$ s. Iso-amplitude lines with relative values are shown. (*c*) Stationary oscillation excited by a wave of half the above period.

Cases where this bay is excited by a stationary sine wave of period $0{\cdot}909 \times 10^{-3}\ K_t$ s and its second harmonic, both coming from the open sea, are shown in figure 23 (*b*) and (*c*).

The case where the bay is disturbed by a pulse-like wave from the open sea is shown by iso-water-level diagrams drawn at regular time intervals $28{\cdot}4 \times 10^{-6}\ K_t$ s in figure 24. This pulse-like wave has a length of about $74 \times 10^{-6}\ K_t$ s and it represents the case of a single, very steep plane wave, with a wave front parallel to the general direction of the coast line, approaching the V-shaped bay. The same phenomena is shown by the vertical sections of the

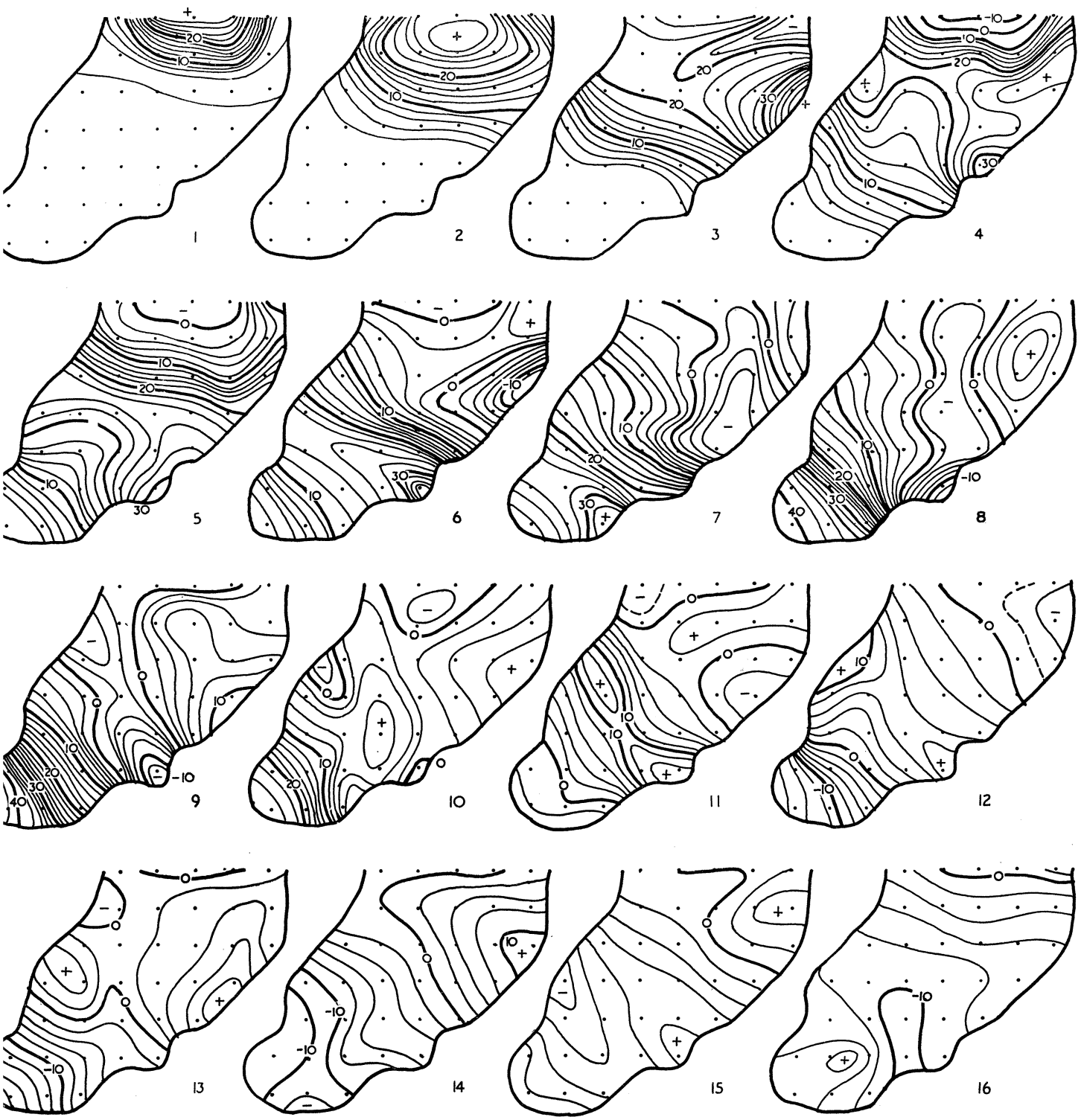

FIGURE 24. Transient state of the water level of the V-shaped bay, shown in figure 23 (*a*), disturbed by a pulse-like wave from the open sea. Diagrams are drawn at regular time intervals ($28{\cdot}4 \times 10^{-6}\ K_t$ s), and iso-water-level lines are shown in each diagram in relative values.

PHILOSOPHICAL TRANSACTIONS OF THE ROYAL SOCIETY A MATHEMATICAL, PHYSICAL & ENGINEERING SCIENCES

water-level variations along the main axis of the bay, taken at the same regular time intervals in figure 25. A section of the topography of the bay along the main axis is also shown in figure 25.

In the same case, the positions of the crests and troughs of the pulse-like wave in the bay, at the same regular intervals of time, are shown in figure 26. In these diagrams, the numbers on the lines show the same times as those indicated in figures 24 and 25. Figure 26 (*a*)

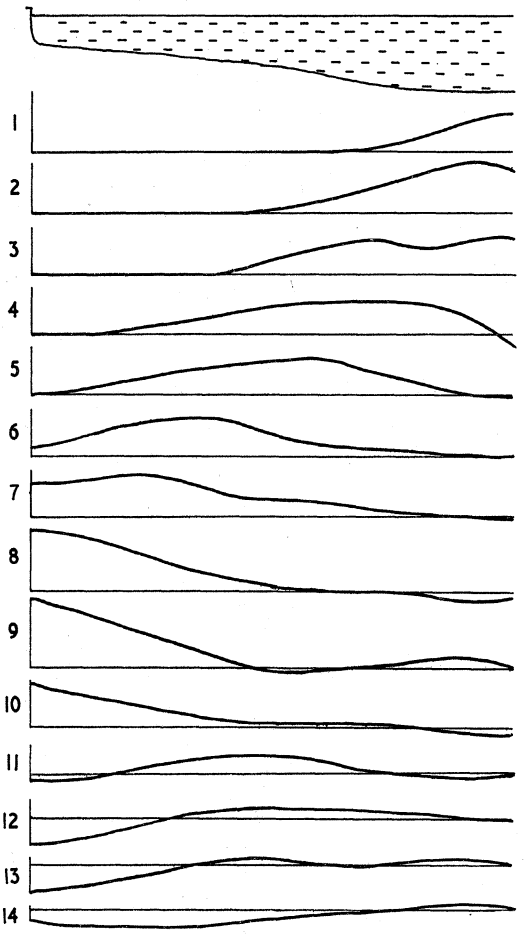

FIGURE 25. Vertical section of the bay shown in figure 23 (*a*) along its main axis (top), and the vertical sections of the water-level variations along this axis (diagrams not on same scale). Numbers show the same times as those indicated in figure 24.

shows the positions of the crest at regular intervals when it is passing from the entrance to the end of the bay; figure 26 (*b*) shows the positions of the crest when the wave is reflected from the end to the entrance. Figures 26 (*c*) and (*d*) show similar positions for the trough. It should be noted that although the physical meaning of these diagrams is similar to ordinary refraction diagrams, the diagrams obtained by the present method include the effects of reflexion and friction as well as refraction.

Although this solution is that of a simple pulse excitation, it is possible, in general to solve for the response to an arbitrary waveform excitation by using the method of § 6·3. An example of the relation between 'unit pulse' (see § 6·3) on the boundary of the bay with open sea and its 'unit responses' on each mesh is shown in figure 27. An example of the

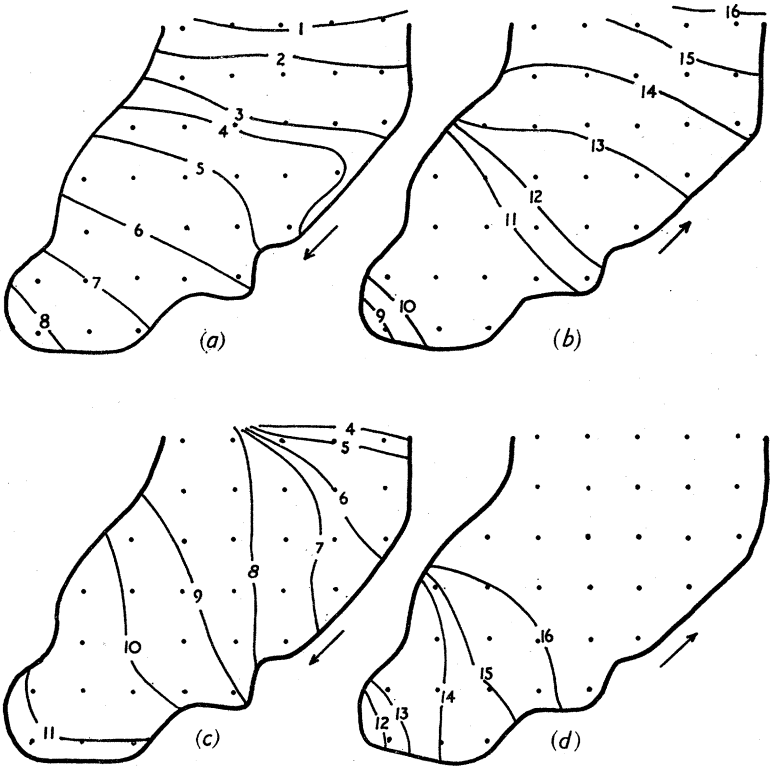

FIGURE 26. Positions of the crests (*a*) and (*b*), and of the troughs (*c*) and (*d*) of the transient oscillations shown in figure 24. Numbers on the lines show the same times as those indicated in figures 24 and 25.

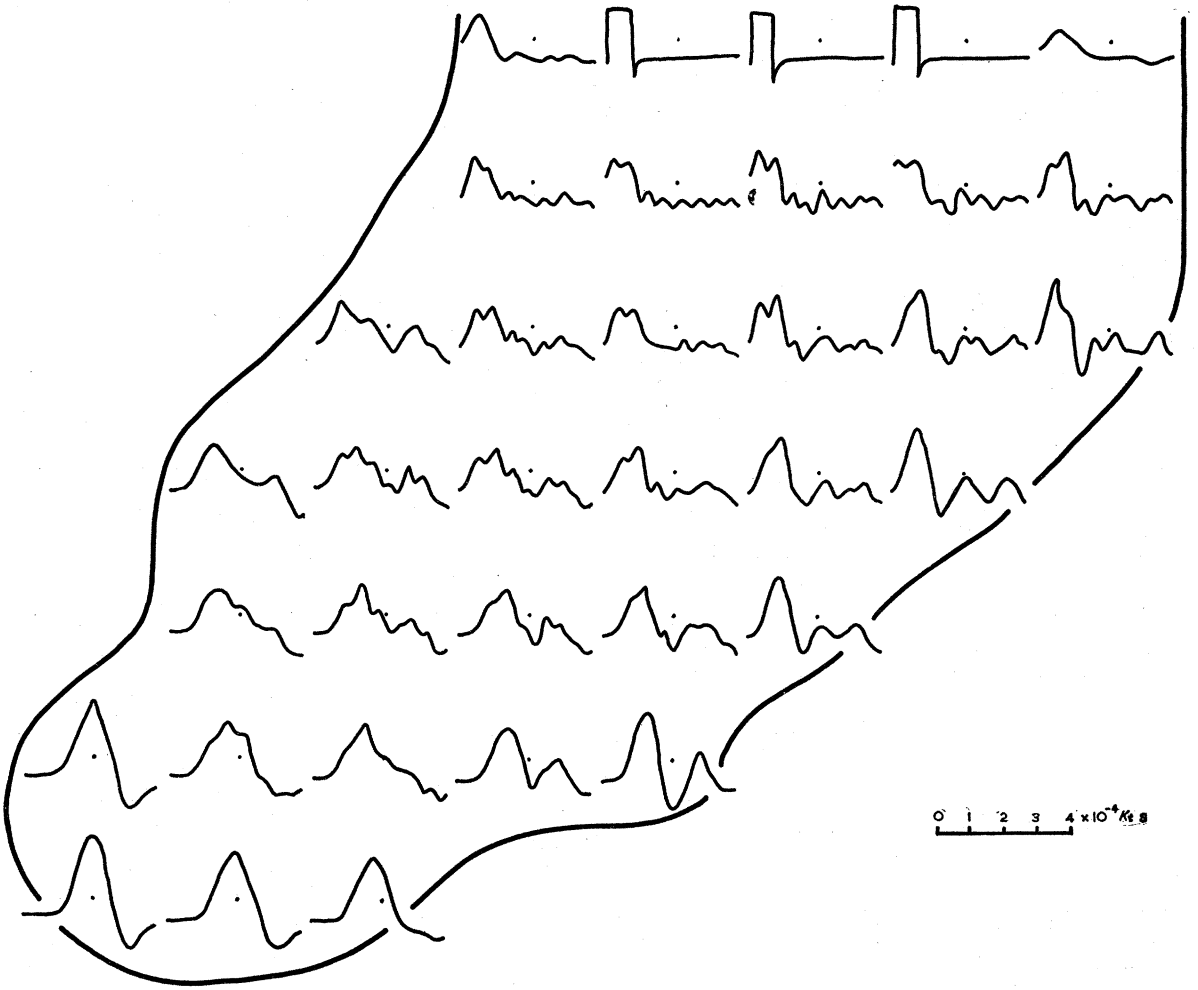

FIGURE 27. 'Unit pulse' put on the boundary of the bay with the open sea, and its 'unit responses' on each mesh. The responses for the first $4 \times 10^{-4}\ K_t$ s, which covers most of the wave duration, are shown in this diagram.

solution for the case where the bay is excited by an arbitrary waveform is shown in figure 28. In this diagram, the response (*d*) on the end of the bay caused by an arbitrary excitation (*c*) on the boundary of the bay is given by the superposition method using a unit pulse (*a*) and its response (*b*).

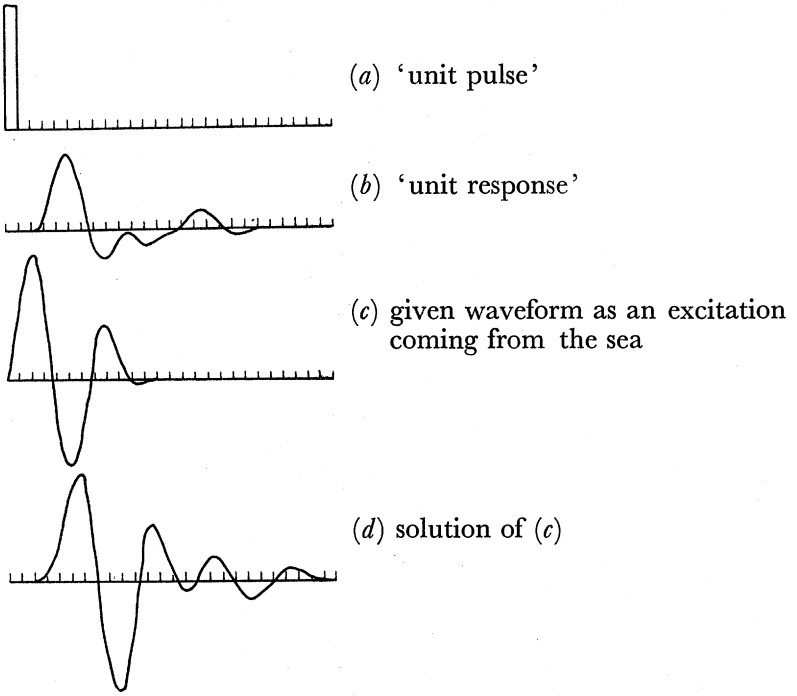

FIGURE 28. Example of the water-level variation at the end of the bay caused by a given arbitrary waveform excitation, obtained by applying the pulse superposition method.

7·4. *Oscillation characteristics of a lake (Lough Neagh)*

A two-dimensional network model of Lough Neagh, a lake in Northern Ireland, was constructed, to investigate the oscillation characteristics of the lake, including those of the transient oscillations caused by the sudden springing up of a wind which affects the water surface two-dimensionally. This lake was chosen as an example for such an investigation because such effects have been studied by means of actual observations on the lake by Darbyshire & Darbyshire (1957).

The principal factors of the model are as follows:

$$n = 39, \quad \Delta l = 3 \text{ km}, \quad K_t = 2 \times 10^8, \quad K_i = 9 \times 10^{11} \text{ cm}^3 \text{ s}^{-1} \text{ A}^{-1},$$
$$K_e = 1 \times 10^2 \text{ cm V}^{-1}, \quad C = 0{\cdot}05 \ \mu\text{F}.$$

The arrangement of the meshes in the lake and the values of the inductances are shown in figure 29. Although the values of the resistances of each mesh arm should be as given by equation (24), the self resistance of each coil had to be used to represent the frictional term, because the values of Q of the present network are rather smaller than those required. Although this may lead to some error in the result, it is adequate to give a qualitative description of the oscillations, and the network can even be applied to transient phenomena if limited to a short duration of time.

Another network having the correct Q values is being designed.

The responses on each mesh caused by a sudden displacement at a point on the lake (A in figure 29), are shown as a time function in figure 30. This diagram can be used for another case where the sudden displacement is made to occur on each mesh point of the lake and the response at point A is required, by applying the reciprocity method. The use of the pulse superposition method will enable the diagram to be used to solve problems where an arbitrary waveform is involved.

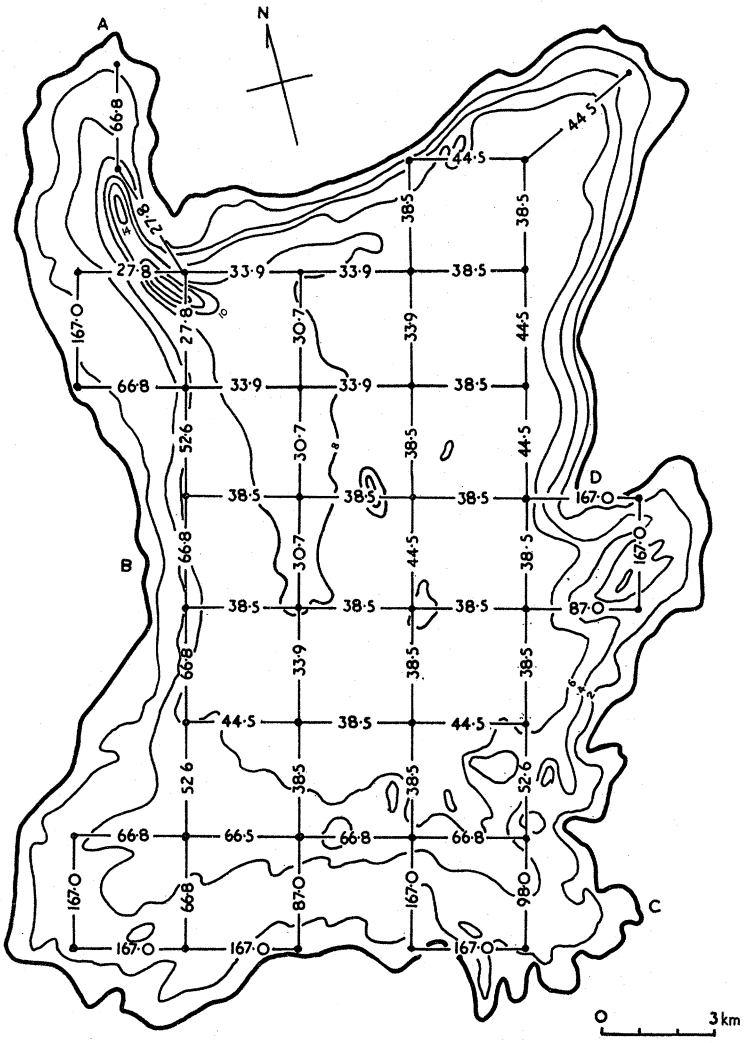

FIGURE 29. Bottom topography of a lake (Lough Neagh) and the arrangement of the meshes. Figures on the contour lines show the depth in fathoms, (2 m), and the figures on the meshes show the values of inductance of the mesh arms in μH. A, Toome Bridge; B, Newport Trench; C, Ellis Cut; D, Langford Lodge.

The transient state caused by a pulse is shown by iso-water-level lines at regular time intervals in figure 31.

Cases where the lake is excited by a stationary sine wave at point A, and also at point C in figure 29, are shown by iso-amplitude lines and by iso-phase lines in figure 32. In all the diagrams in figure 32, the periods of the excitation waves were adjusted to give a phase

difference of 180° between the points A and C and this was given by a period of 1·64 h. This value is in good agreement with that obtained by Darbyshire & Darbyshire (1957), by Fourier analyzing the full-scale observations. Although the same technique was applied at other points on the lake, such good agreement was not obtained with the full-scale observations. This is because the period would be less and, as shown in figure 4, the accuracy decreases with the period.

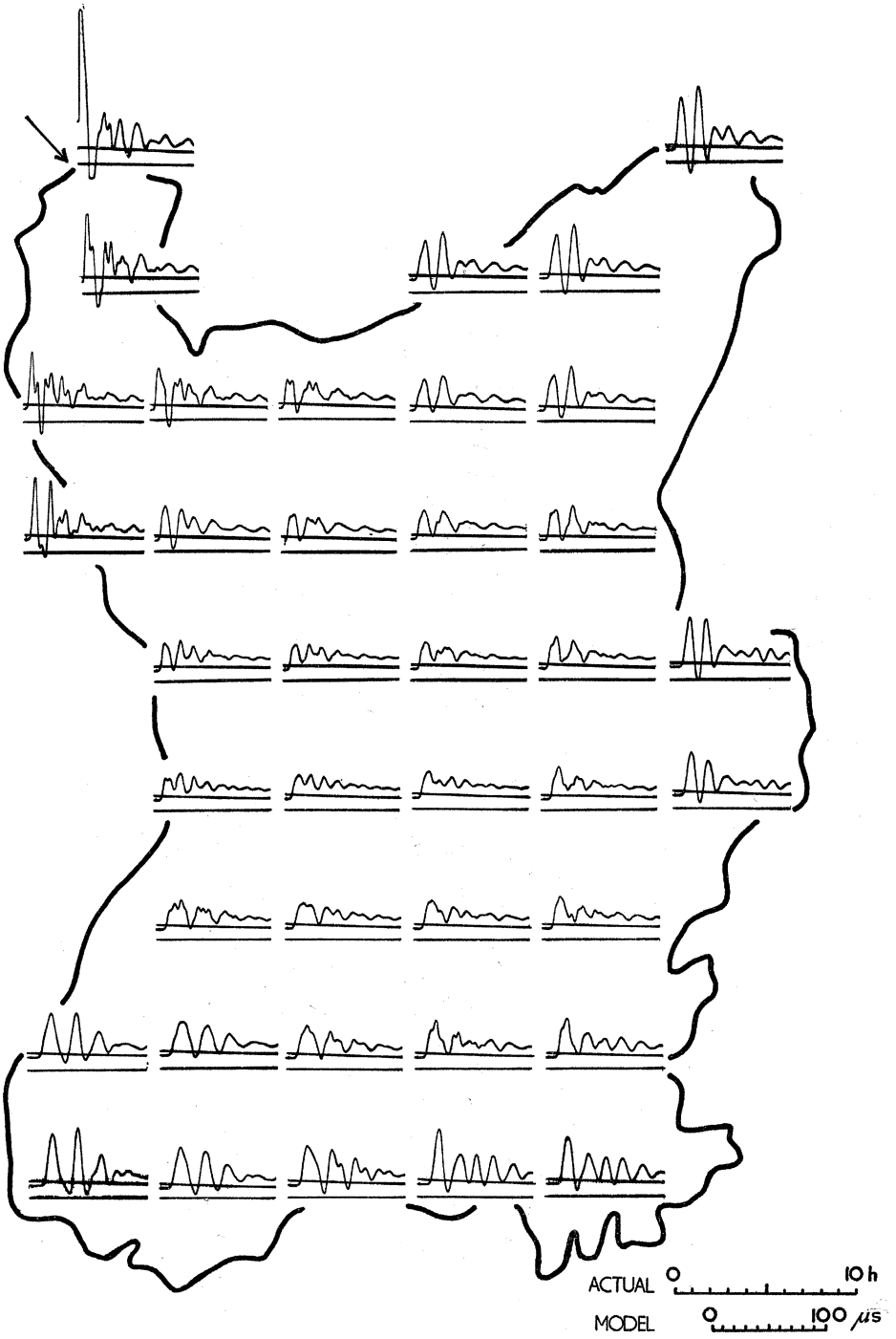

FIGURE 30. Responses on each mesh caused by a sudden displacement at a point (shown by arrow) on the lake.

PHILOSOPHICAL TRANSACTIONS OF THE ROYAL SOCIETY A MATHEMATICAL, PHYSICAL & ENGINEERING SCIENCES

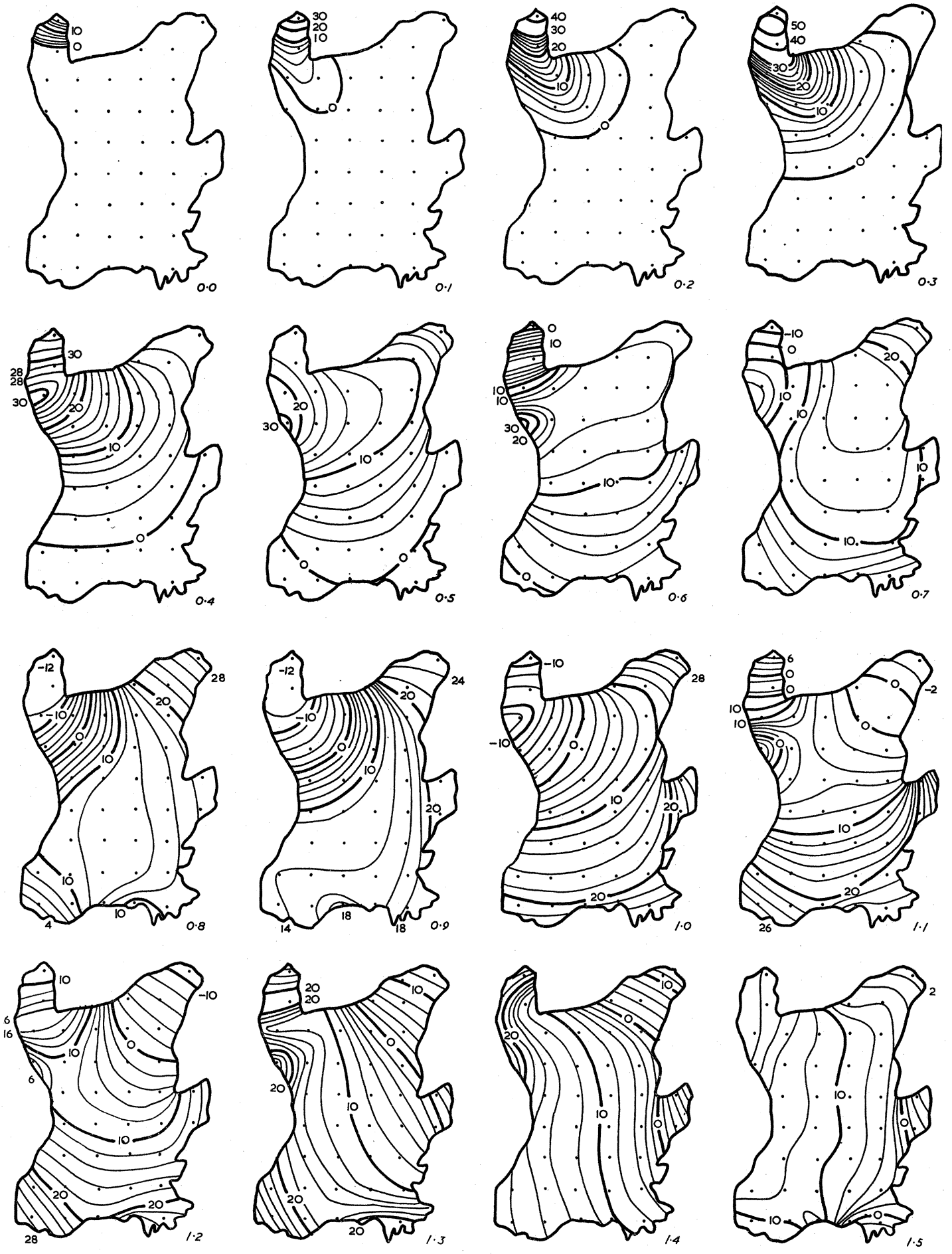

FIGURE 31. For legend see p. 335.

PHILOSOPHICAL TRANSACTIONS OF THE ROYAL SOCIETY A MATHEMATICAL, PHYSICAL & ENGINEERING SCIENCES

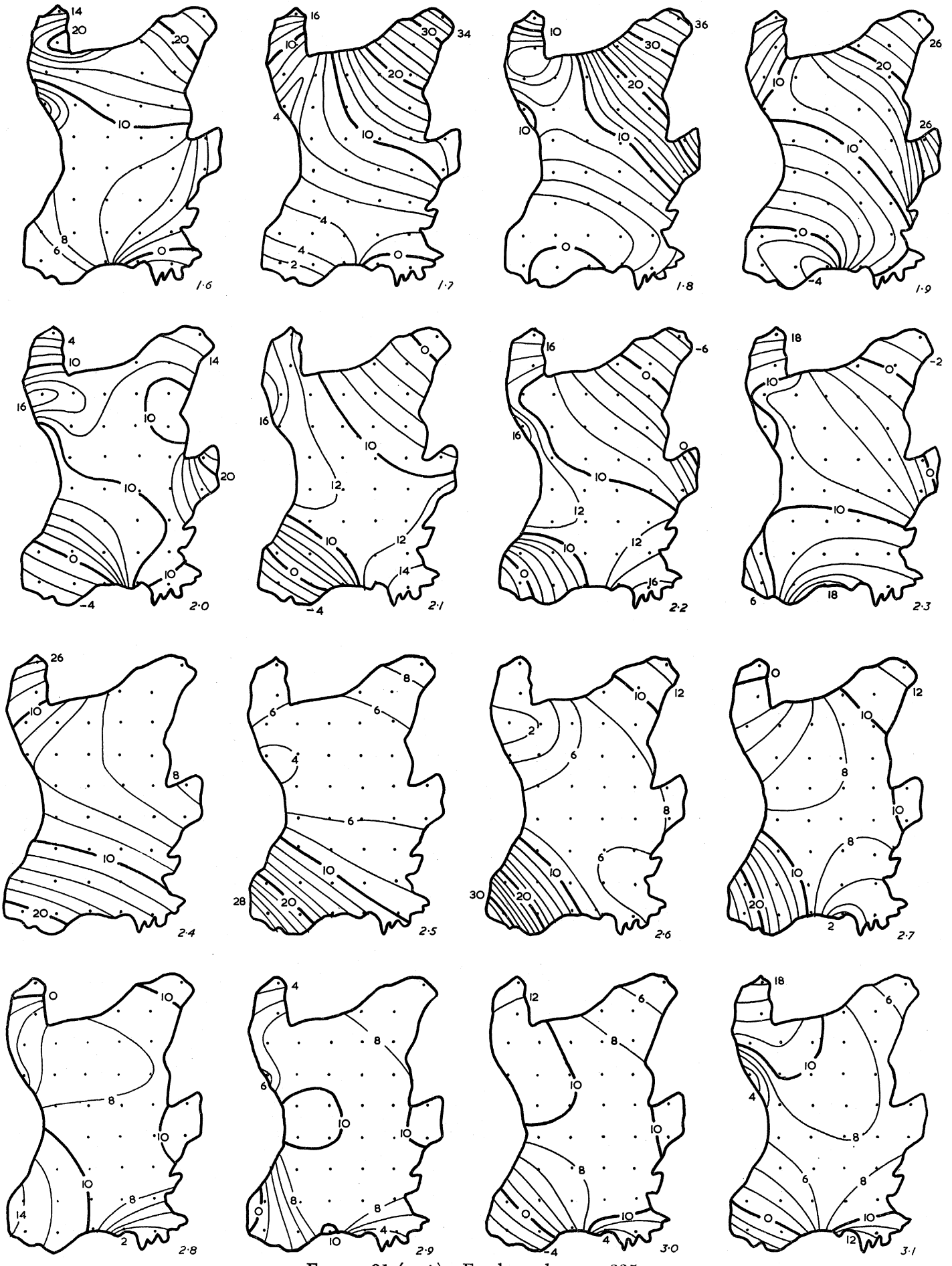

FIGURE 31 (*cont.*). For legend see p. 335.

PHILOSOPHICAL TRANSACTIONS OF THE ROYAL SOCIETY A MATHEMATICAL, PHYSICAL & ENGINEERING SCIENCES

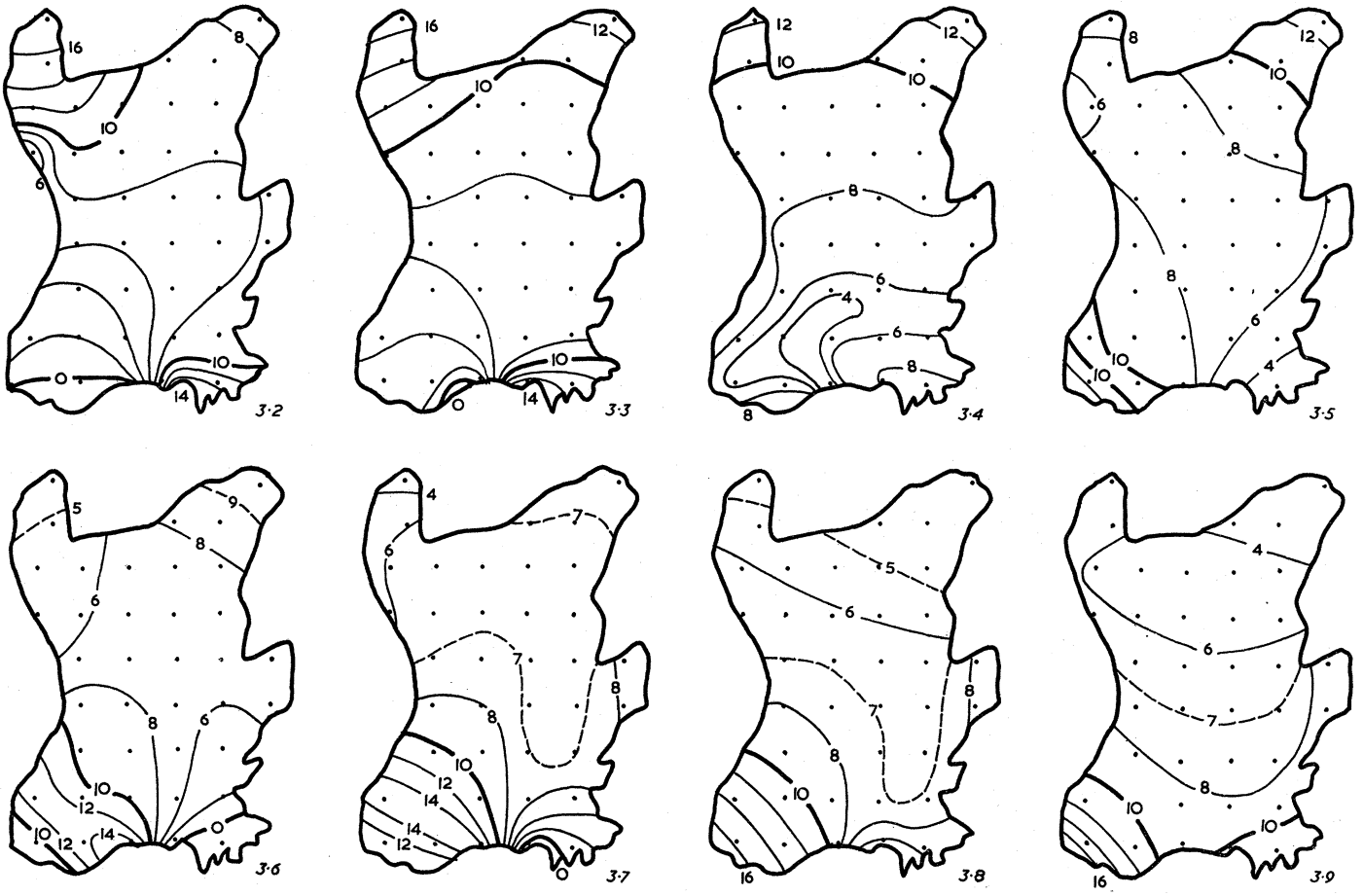

FIGURE 31 (*cont.*). Transient state of the water level of Lough Neagh disturbed by a pulse. Diagrams are drawn at regular time intervals (0·1 h in actual time units), and iso-water-level lines are shown in each diagram in relative values.

To investigate the way free oscillations are propagated in the lake, the method described in § 6·2 and figure 13 (*b*) was applied. In figure 33, a pulse is injected at all the mesh points indicated by circles to start the free oscillations. The position of these points and the pulse lengths were selected so that the oscillations caused would be as simple as possible. Pulse lengths of 1 and 0·62 h (in actual time units) are used for the case shown in figure 33 (*a*) and (*b*), or (*c*) and (*d*). Lines showing the position of the crests of pulse-like waves at regular time intervals are shown in (*b*) and (*d*), the numbers indicating the time from the instant of injection in actual time units. It should be noted that although the positions of crests reflected from the opposite coast can be obtained by the same procedure, these are not shown in these diagrams. The displacement of water level caused by the same pulse are shown in (*a*) and (*c*).

The 'frequency response curve' (see § 6·5) of the lake, obtained by exciting point A, is shown in figure 34.

In this lake, the amplitude of the seiches was found by Darbyshire & Darbyshire (1957) to be closely related to the product of the wind speed and the rate of change of wind direction. This phenomenon was analyzed by using the network model and the method described in 6·4 (C) and figure 16. An example of this effect was taken, the observational

data from 19.00 to 01.00 G.M.T., 16 to 17 April 1949. The wind direction and speed, and the water-level variation at Toome Bridge (corresponding to point A in figure 29), are shown in the top part of figure 35 (*a*). Finite intervals of time ('time sections') are considered, and the mean square wind speed during each time section is computed. Pulses proportional in height to this mean square wind speed, and in duration equivalent to the time

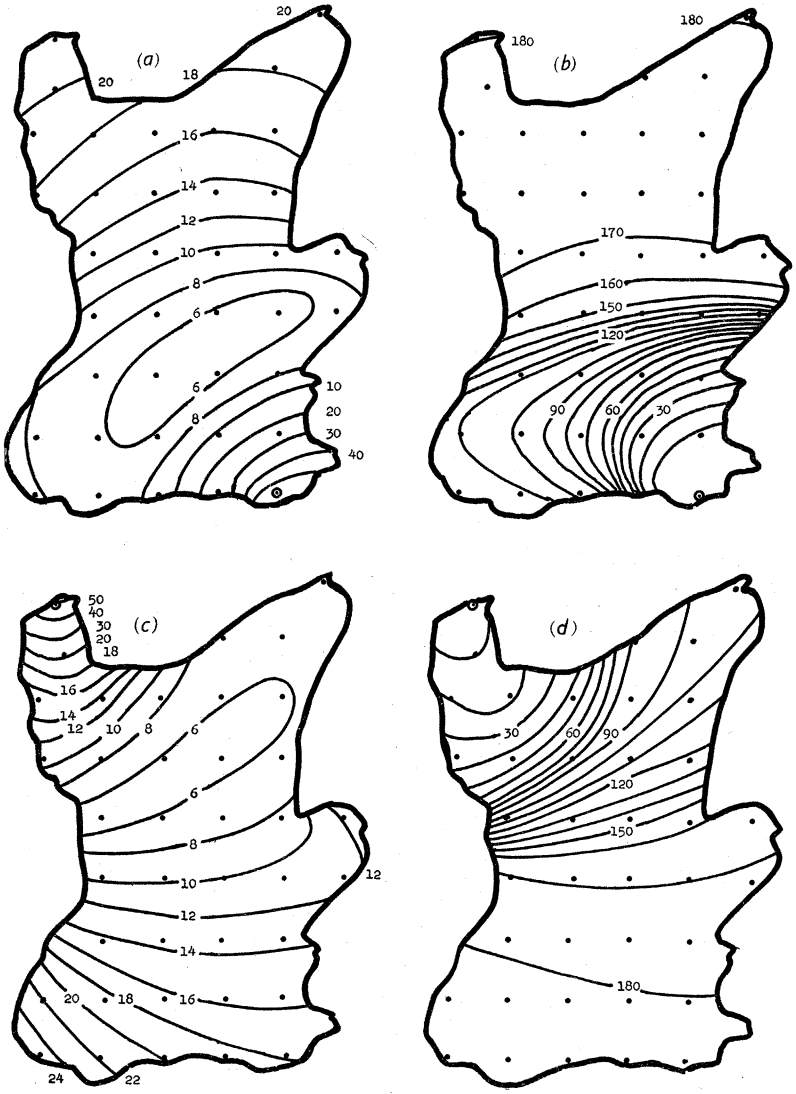

FIGURE 32. Stationary oscillations excited by a sine wave at a point (shown by circule) on the lake. (*a*) and (*c*) Iso-amplitude lines based on relative values. (*b*) and (*d*) Iso-phase line in degrees.

interval, are injected into the network at positions chosen from seventeen meshes near the perimeter of the lake as shown in figure 35 (*b*). For each time section, two groups of five meshes at opposite sides of the lake are selected, and for successive time sections, these are chosen in rotation round the perimeter so that the effect of variation of wind direction is simulated. The actual response is obtained in each case by injecting a pulse at point A and superposing the responses obtained on the two sets of five meshes. The variation in wind direction is represented by a vector in figure 35 (*b*). The response on each group of meshes is shown in (*a*), the numbers corresponding to the mesh numbers shown in (*b*). All these

responses are superposed shifting the time axes according to the position of the time sections. It is assumed that the downwind side of the lake gives a positive response, and the upwind side a negative response, so that responses from meshes 1 to 8 are superposed positively and responses from meshes 9 to 17 are inverted before superposition. The results

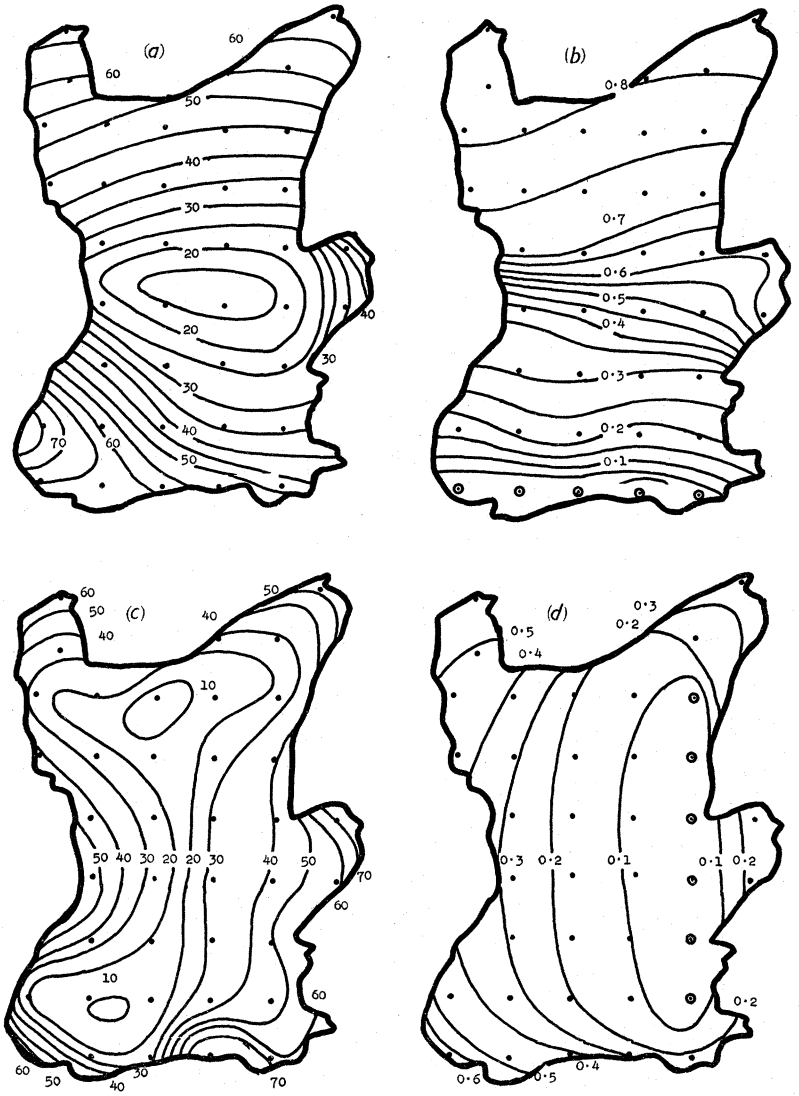

FIGURE 33. Free oscillations of the lake caused by a pulse at a group of points (shown by circles). (*a*) and (*c*) Displacement of water level in relative values. (*b*) and (*d*) Lines showing the position of the crests every 0·1 h.

obtained by superposing all the responses in this manner is shown in the bottom of figure 35 (*a*). This curve represents the water-level variation and is very similar to the curve of actual observations shown in the top of figure 35 (*a*). It should be observed that considering the limits set to accuracy of the present network, the agreement is satisfactory. It is also clear that the analogue method enables a detailed study to be made of the actual mechanism of the effect of the wind on the water surface.

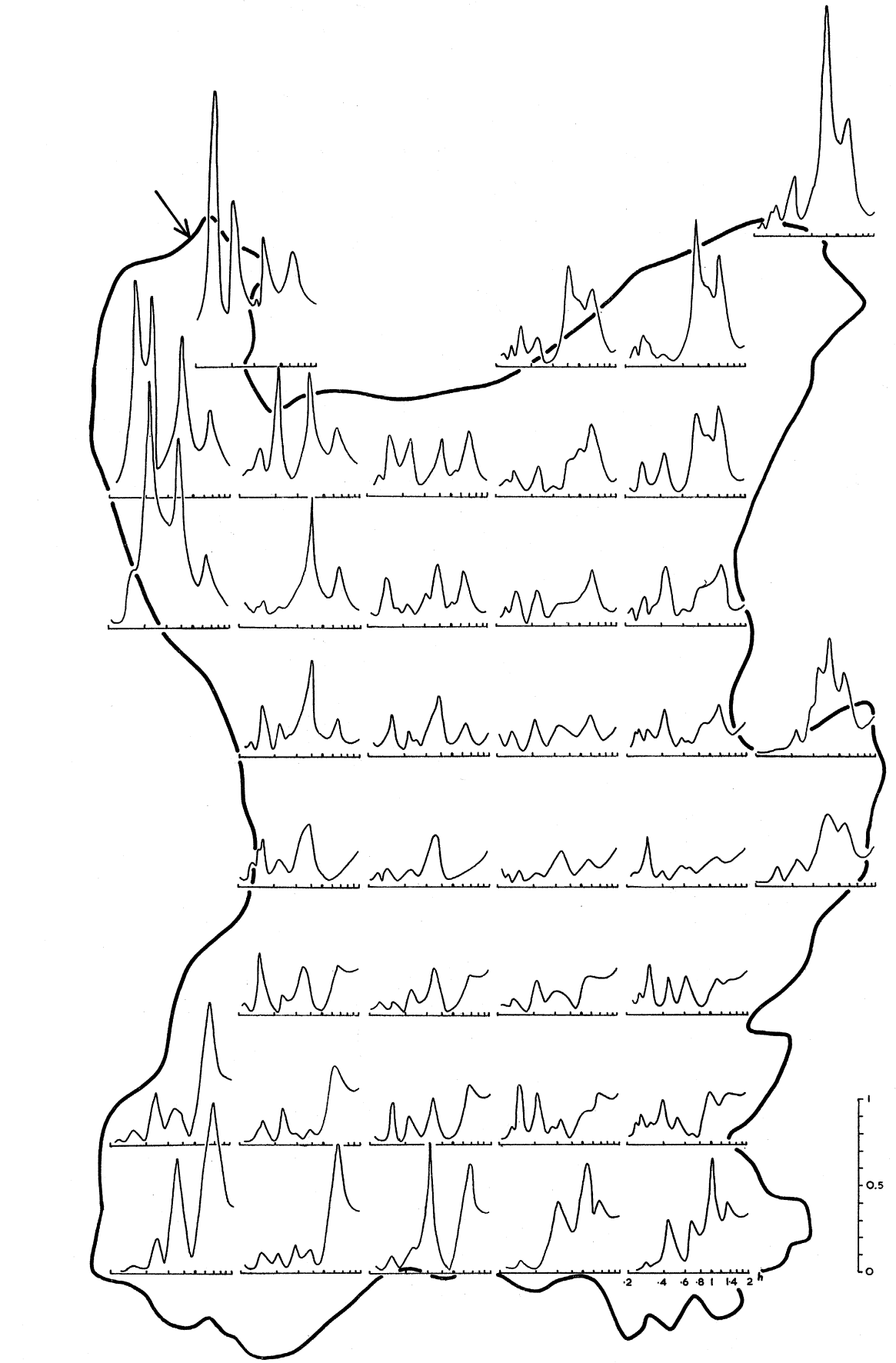

FIGURE 34. 'Frequency response curve' (see § 6·5) of Lough Neagh, obtained by exciting a point (shown by arrow) by a sine wave of constant amplitude and various frequencies. The sine wave periods measured in hours are shown on the horizontal scale, and the ratios of the response amplitudes to the exciting amplitude are shown on the vertical scale.

PHILOSOPHICAL TRANSACTIONS OF THE ROYAL SOCIETY A MATHEMATICAL, PHYSICAL & ENGINEERING SCIENCES

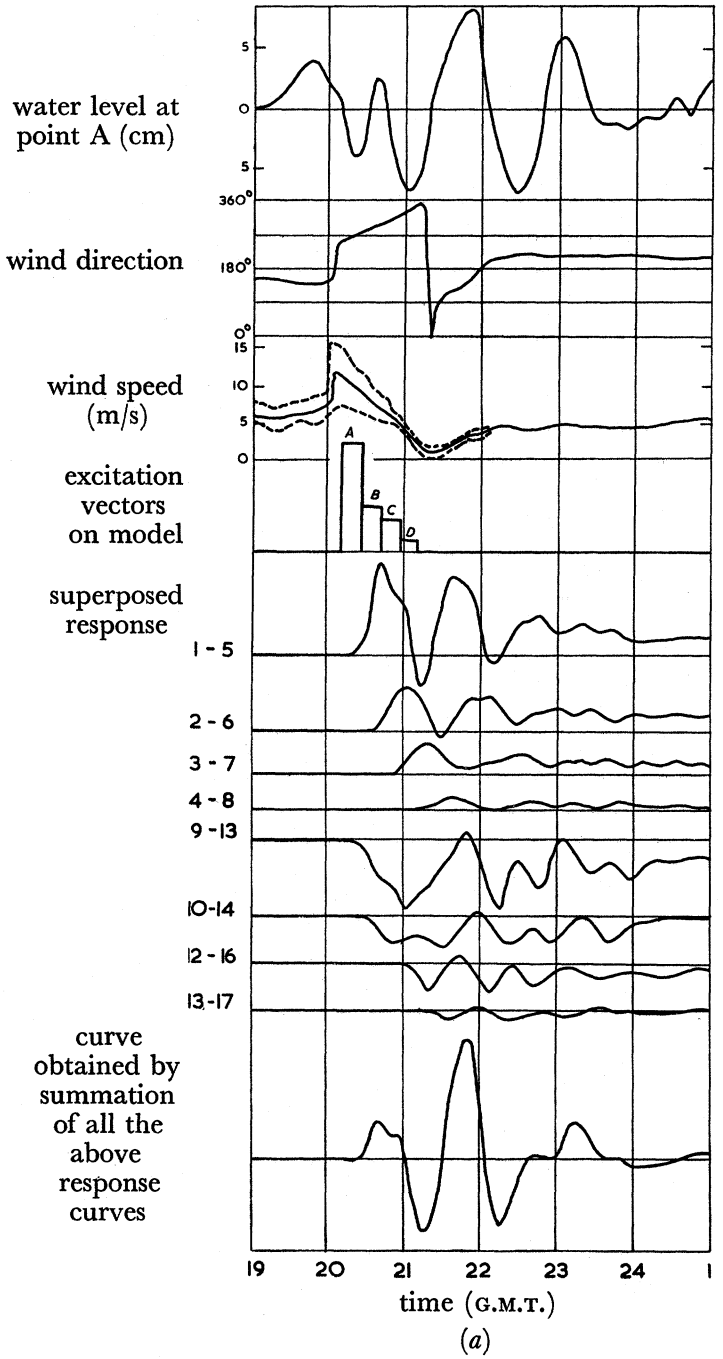

(a)

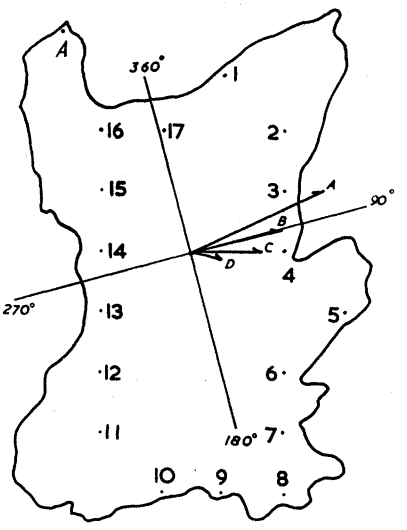

(b)

FIGURE 35(*a*). Analysis and comparison of the transient state of the seiches caused by the variation of wind speed and direction in a lake (Lough Neagh) and its electric network model.

FIGURE 35(*b*). Vectors representing the wind stress, and points of the meshes of the network model used for the analysis shown in figure 35(*a*). The numbers on them correspond to those in figure 35(*a*).

8. Conclusions

The closeness of the results obtained by the electronic analogue method with those obtained on full scale shows that it is a very powerful tool in investigating long-wave phenomena. The success gained by the relatively simple model encourages the construction of more complicated models, (*a*) with a larger number of meshes, (*b*) taking into account the earth's rotation, and (*c*) using very high Q coils which can represent phenomena with a small loss of energy.

This study was started by the author in 1949 (Ishiguro 1950) at the Nagasaki Marine Observatory, Nagasaki, and is being carried on at present at the British National Institute of Oceanography, with financial support from U.N.E.S.C.O. and also the Scripps Institution of Oceanography, La Jolla, through the Japanese Organization for Tsunami Investigations, Tokyo.

The author wishes to express his thanks to Professor S. Kaya, Professor K. Hidaka and Professor R. Takahashi of Tokyo University, Professor M. Uda of Tokyo University of Fisheries, and Dr K. Wadati and Dr M. Nakano of Japan Meteorological Agency, for kind help and encouragement.

The author also wishes to express his thanks to the Director, Scripps Institution of Oceanography, and the Director-General and Director of the Natural Sciences Department of U.N.E.S.C.O. for their strong support for the continuance of this study.

Finally, the author wishes to thank Dr G. E. R. Deacon, F.R.S., Mr M. J. Tucker, Dr and Mrs J. Darbyshire and many other members of the National Institute of Oceanography for their kind guidance, advice and invaluable help.

References

Bowden, K. F. 1956 *Phil. Trans.* A, **248**, 517.
Darbyshire, J. & Darbyshire, Mollie 1957 *Quart. J.R. Met. Soc.* **83**, 93.
Ishiguro, S. 1950 *Oceanogr. & Met., Nagasaki*, **4**, 59.
Proudman, J. 1953 *Dynamical Oceanography*. London: Methuen.
Rossiter, J. R. 1953 *Phil. Trans.* A, **246**, 371.

PHILOSOPHICAL TRANSACTIONS OF THE ROYAL SOCIETY A MATHEMATICAL, PHYSICAL & ENGINEERING SCIENCES

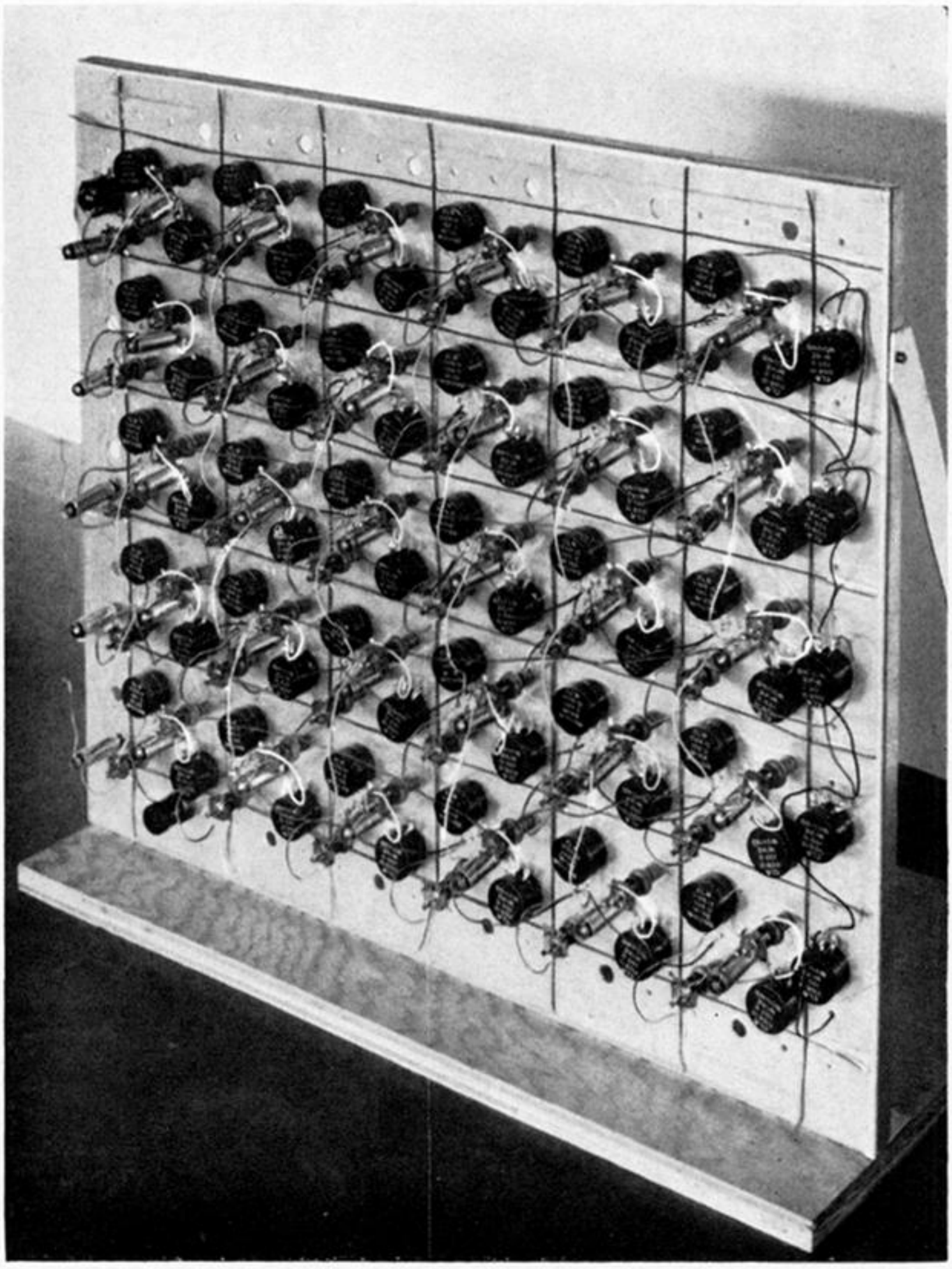

FIGURE 8. Example of a 30-mesh network.

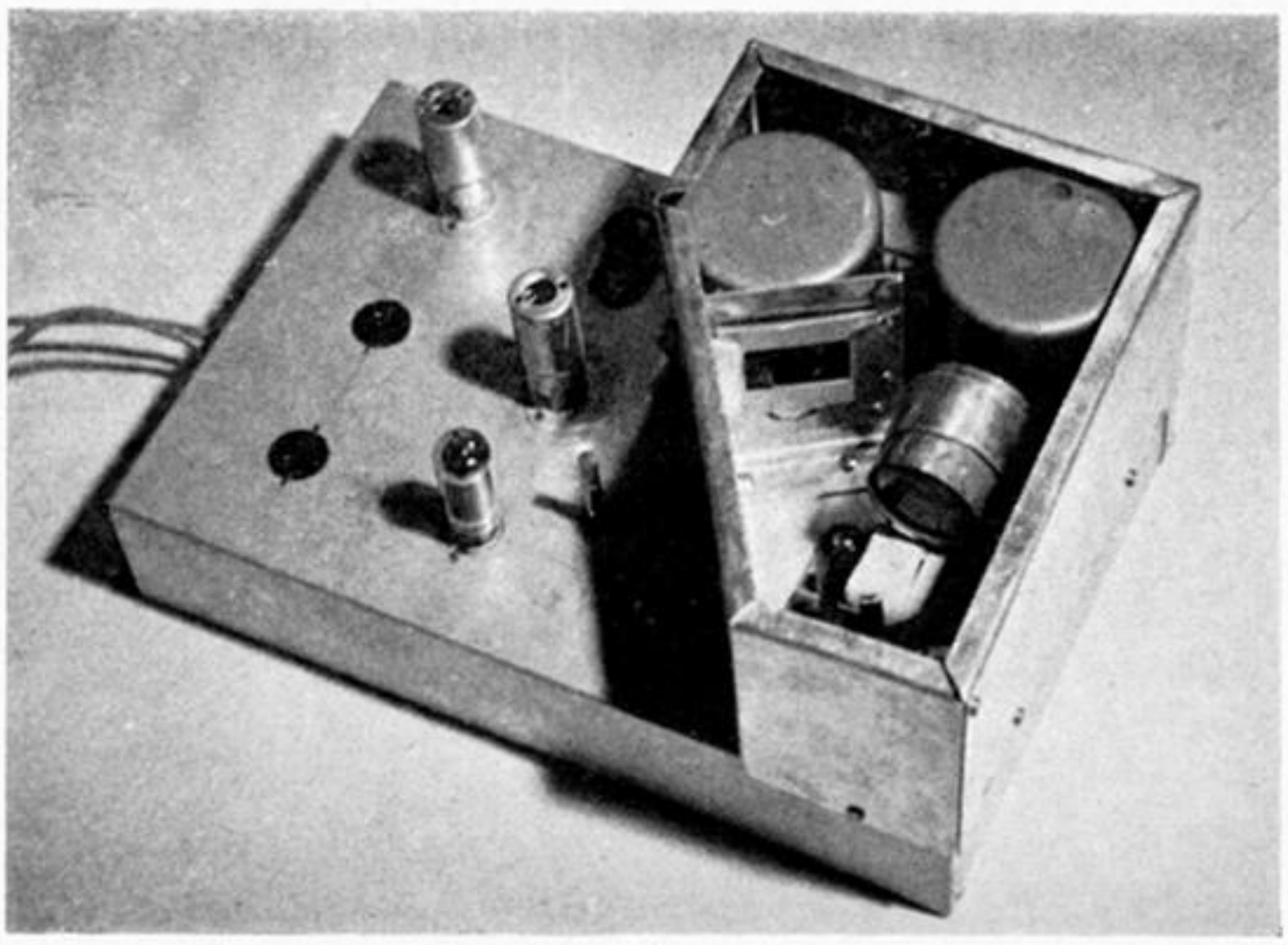

FIGURE 10. Example of an arbitrary waveform generator for a low-frequency range.

PHILOSOPHICAL TRANSACTIONS OF THE ROYAL SOCIETY A MATHEMATICAL, PHYSICAL & ENGINEERING SCIENCES